ANALYSIS OF DNA DOUBLE-STRAND BREAK REPAIR GENES *RAD50* AND *XRCC2* USING ZEBRAFISH AS THE MODEL SYSTEM

by

Alex William Stark

A dissertation submitted to the faculty of
The University of Utah
in partial fulfillment of the requirements for the degree of

Doctor of Philosophy

Department of Oncological Sciences

The University of Utah

May 2018

The University of Utah Graduate School

STATEMENT OF DISSERTATION APPROVAL

The dissertation of **Alex William Stark**

has been approved by the following supervisory committee members:

Sean Vahram Tavtigian	, Chair	**Dec. 11, 2017** Date Approved
David Grunwald	, Member	**Dec. 11, 2017** Date Approved
Rodney A. Stewart	, Member	**Dec. 11, 2017** Date Approved
Joshua David Schiffman	, Member	**Dec. 11, 2017** Date Approved
Srividya Bhaskara	, Member	**Dec. 11, 2017** Date Approved

and by **Bradley Cairns** , Chair/Dean of

the Department/College/School of **Oncological Science**

and by David B. Kieda, Dean of The Graduate School.

ABSTRACT

DNA double-strand break (DSB) repair gene products play an important role in development and tumor suppression. Mutations in *ATM*, *BRCA1*, *BRCA2*, *MRE11*, *NBN*, *PALB2*, *RAD50*, *RAD51*, and *XRCC2* result in embryonic lethality or cause pediatric diseases including ataxia-telangiectasia, Fanconi anemia (FA), Nijmegen breakage syndrome (NBS), and other disorders.

A DNA DSB can be repaired using two different pathways: nonhomologous end-joining (NHEJ) and homology-directed DSB repair (HDR). Some DSB repair proteins, including ATM, Mre11, RAD50, and Nibrin, function in both pathways. RAD51 and its paralogs only function in HDR.

Mre11-Rad50-Nibrin (MRN) complex is a heterohexamer composed of dimers of each protein. The MRN complex is important for early detection of DNA DSBs and activates downstream effectors, most notably the protein kinase ATM. ATM phosphorylates other DNA repair proteins including H2AX. γH2AX, phosphorylated histone H2AX, is an important DNA damage signaling factor that helps recruit BRCA1 to damaged DNA. XRCC2 helps promote RAD51 foci through interaction with other RAD51 paralogs RAD51B, RAD51C, and RAD51D to form the BCDX2 complex.

FA and NBS-like disorder result from biallelic mutations in *XRCC2* and *RAD50*, respectively. These genetically distinct disorders share many clinical similarities. Bone marrow failure is a key symptom of FA and has been observed in multiple NBS patients.

The hematopoietic malignancy acute myeloid leukemia has been observed in patients suffering from FA and NBS. Hormone abnormalities and fertility issues present in both patient populations as do issues with growth and development.

Null mutations in *RAD50* and *XRCC2* are embryonic lethal in humans and mice, so zebrafish was chosen as the model organism to study mutations in each of these genes. Null mutations in related genes (e.g., *BRCA2*) that result in embryonic lethality in humans and mice are tolerated in zebrafish. Frameshift mutations were generated in *rad50* and *xrcc2* using transcription activator-like effector nucleases in zebrafish. We recovered the first viable vertebrate model for biallelic null mutations in *RAD50* and *XRCC2*. Study of these mutants might offer unique insights into human disease that have not been possible previously due to a lack of appropriate model systems.

TABLE OF CONTENTS

LIST OF FIGURES

Figures

ACKNOWLEDGMENTS

Finishing graduate school would not have been possible without the constant love and support of my wife Crystal Stark. Having our son, Theodore Stark, during graduate school was a wonder experience. I also could not have gotten through graduate school without the rest of my family, including my parents, Jeff and Maria Stark, and my brother Aaron Stark. Lastly, I would like to thank Dr. Sean Tavtigian, my mentor, the rest of the Tavtigian lab, and my thesis committee for helping me with experimental design, data collection, and writing. Within the Tavtigian lab, I would like to highlight Andrew Paquette, a fellow graduate student and Jessie Duarte, an undergraduate lab assistant. They both helped me so much through graduate school, and I would not have wanted to go through the process without them.

CHAPTER 1

INTRODUCTION

Many breast cancer susceptibility genes are members of the DNA double-strand break (DSB) repair pathway [1]. Proteins encoded by genes including *ATM*, *BRCA1* and *BRCA2*, the Mre11-Rad50-NBN (MRN) complex genes, and *RAD51* and its paralogs play a central role in the proper repair of DNA double-strand breaks (DSBs) [1]. Homozygous mutations in many of these genes result in embryonic lethality in both humans and mice or severe childhood diseases such as ataxia-telangiectasia (A-T), Fanconi anemia (FA), and Nijmegen breakage syndrome (NBS), which makes it difficult to study the roles these genes play in development [2].

DNA double-strand break repair

There are two main pathways for repair of DNA DSBs: nonhomologous end-joining (NHEJ) and homology-directed DSB repair (HDR) [3–5]. NHEJ does not require a sister chromatid for repair [3]. As a result, repair is much more error prone, often resulting in indel and point mutations [3]. HDR is much less error prone because it uses the sister chromatid as a template for repair [5]. Because NHEJ does not require a sister chromatid while HDR does, cells in G_0/G_1 can only utilize NHEJ for repair of DSBs [6]. The MRN complex acts early enough in the double-strand break repair pathway that it is involved in

both NHEJ and HDR, while the FA genes, *BRCA1*, *BRCA2*, *BRIP1*, *PALB2*, *RAD51*, *RAD51C*, and *XRCC2*, are only involved in HDR [3–5].

An essential protein complex for detection of DNA DSBs is the Mre11-Rad50-Nibrin (MRN) complex [7,8]. The MRN complex is composed of protein dimers of Mre11, RAD50, and Nibrin [9]. *Mre11* and *Rad50* are conserved in both prokaryotes and archaea [10]. There are four key domains within the MRN complex: the head, coil, hook, and flexible adapter domains [9]. The head domain is composed of a dimer of Mre11 and the ATPase domains (Walker A and Walker B) from both RAD50 proteins [9]. The coil and hook domains are both composed from Rad50 protein sequence, with the hook domain also containing zinc ions [9]. Last, the flexible adapter connects the head domain to Nibrin and to the important signaling functions of MRN [9,11]. Disruption of any of these domains can severely impact MRN function. Mre11 functions in binding to damaged DNA, and additionally has exo- and endonuclease activity [9,12,13]. Rad50 serves important structural roles in the MRN complex through conformational changes due to ATP binding and long-range tethering of damaged DNA [7,8,14,15]. Through its forkhead-associated domain (FHA) and BRCT domain, Nibrin helps to correctly localize the MRN complex and activate downstream effectors, notably ataxia-telangiectasia mutated (ATM) [16–18].

In response to DNA damage, ATM is recruited to the break site by Nibrin [11,18]. In the absence of Nibrin, ATM can phosphorylate H2AX and only transiently phosphorylate p53 but cannot phosphorylate its other targets, including Chk2 and BRCA1 [11,19,20]. This canonical activation has been challenged by recent evidence that ATM can be activated by Ku and DNA-PKcs in the absence of the MRN complex [20]. ATM is the main mediator of histone H2AX phosphorylation, denoted γH2AX, necessary for proper

recruitment of BRCA1 and other proteins to break sites [21,22]. H2AX phosphorylation is also modestly important for the recruitment of the MRN complex members (You et al., 2010). ATM also phosphorylates Chk2 at Thr^{68}, which induces polymerization of Chk2, causing *trans*-phosphorylation at Thr^{383} and Thr^{387}, producing activated Chk2 [23]. Activated Chk2 induces cell cycle arrest through phosphorylation of Cdc25A and Cdc25C [24,25]. Chk2 also can then phosphorylate BRCA1 at Ser^{988}, which activates the HDR pathway [26]. BRCA1 is also phosphorylated by ATM in response to DNA DSBs [27].

BRCA1 and BARD1 heterodimerize through their RING domains [28]. This interaction stabilizes each protein and facilitates early recruitment of BRCA1 to the sites of DSBs through the interaction between the BARD1 BRCT domain and poly(ADP-ribose) [29,30]. BRCA1 interacts with RAD51 at the sites of DNA damage [31]. These foci are marked by γH2AX, which is responsible for the recruitment of many factors to the DNA break site [32,33]. The exact role that BRCA1 plays at the site of DNA damage is not yet fully known. One hypothesis is that BRCA1 acts as a scaffold for ATM-ATR signaling [34,35]. Through interaction with RAD51, BRCA2 mediates strand invasion [36]. PALB2 facilitates the interaction between BRCA1, BRCA2, and RAD51 at the DNA damage site [37].

XRCC2, which is one of the five *RAD51* paralogs, helps promote HDR [38]. The other *RAD51* paralogs include *RAD51B*, *RAD51C*, *RAD51D*, and *XRCC3* [38]. Each paralog is nonredundant and is necessary for HDR [38–41]. *XRCC2* was first identified for its ability to complement hypersensitivity to DNA damaging agents seen in the irs1 Chinese hamster ovary cell line [42,43]. XRCC2 interacts with other RAD51 paralogs RAD51B, RAD51C, and RAD51D to form the BCDX2 complex, which promotes

RAD51 foci formation [44–49]. The CX3 complex, composed of RAD51C and XRCC3, acts downstream of the BCDX2 complex and helps resolve Holliday junctions, a key intermediate in homologous recombination [41].

Loss of DSB genes results in severe genetic disorders

Biallelic mutations in *RAD50* and *XRCC2* result in the genetic disorders NBS-like disease and FA, respectively [50–52]. While NBS-like disease and FA are distinct genetic disorders, there are overlapping clinical features between the two diseases [53]. Bone marrow failure has been reported in several NBS patients and is a key feature in FA [54–57]. Acute myeloid leukemia (AML) develops in patients suffering from each disease as well [54,58–60]. Patients suffering from FA or NBS exhibit growth retardation, microcephaly, and defects of the thumbs [53,61–67]. Female FA and NBS patients both present with primary ovarian insufficiency [68,69]. Hormone abnormalities are also observed in both FA and NBS patients, including elevated follicle stimulating hormone (FSH) levels [69,70].

NBS and NBS-like disease

The MRN complex and downstream target ATM all result in diseases with similar cellular phenotypes when the genes are mutated. A-T is caused by biallelic mutations in *ATM* [71]. Biallelic *MRE11* mutations cause the related A-T-like disorder [72]. Biallelic mutations in *NBN* and *RAD50* result in the similar diseases NBS and NBS-like disorder, respectively [50,61,62]. Given the interactions between these genes, it is not surprising that they share many cellular phenotypes. Chromosomal instability, radiosensitivity, radioresistant DNA synthesis, and defective G_1/S and G_2/M checkpoints are all hallmarks

of both NBS and NBS-like disorder at the cellular level [73]. A-T patients suffer from ataxia, which is loss of motor control, and telangiectasia, a condition characterized by dilated blood vessels below the skin [73]. These symptoms, in addition to cerebellar degeneration, are not present in NBS patients [61,62,73]. A-T patients do share some symptoms with NBS patients, namely ovarian dysgenesis, immunodeficiency, cancer predisposition, and growth retardation, though to a lesser extent than what is seen in NBS patients [73].

Homozygous null *RAD50* mutations are lethal in mice [74]. One human patient presented with NBS but did not carry two mutant alleles in *NBN* [50,75]. Instead, this patient, who was not the result of a consanguineous marriage, carried two different *RAD50* mutations, a nonsense mutation (c.3277C→T; p.R1093X) and a loss of the stop codon (c.3939A→T) [50]. The patient presented with less than 5% RAD50 protein level compared to wild type [50]. Most of our knowledge about NBS comes from patients with *NBN* mutations because there currently exists only one human patient that presented with biallelic *RAD50* mutations, and this patient is likely only able to survive because they do not have a complete loss of *RAD50*. A founder mutation (c.657_661del5) exists in *NBN* in Slavic populations, making the disease most common in those populations [67]. We know from NBS patients that issues with the hematopoietic system exist, namely two cases of bone marrow aplasia in unrelated Russian NBS patients and aplastic anemia in a Japanese child with NBS [54,55]. These findings of bone marrow defects are observed in a mouse model that contains a hypomorphic *Rad50* mutant allele, dubbed the *Rad50*S allele [76,77]. *Rad50*$^{S/S}$ mice show growth retardation that is due to hematopoietic failure, and one mouse developed myeloid leukemia, a cancer type observed in human NBS

patients [54,76]. These findings illustrate that mouse hypomorphic *Rad50* mutants show multiple phenotypes consistent with human NBS, further supporting that biallelic *RAD50* mutations cause NBS-like disease.

Fanconi anemia

FA is a genetic disease caused by mutations in any of 21 different genes involved in DNA interstrand cross-links (ICL) repair or HDR [52,78–82]. Nineteen of the genes act as autosomal recessive genes, while *FANCB* is the lone X-linked recessive FA gene and *RAD51* (*FANCR*) is the lone autosomal dominant FA gene [79,80,83]. As mentioned previously, FA is genetically distinct from NBS, yet both diseases share many common symptoms.

Repair of interstrand cross-links is the least understood form of DNA repair for two main reasons: the difficulty in creating cross-links to study, and the fact that different cross-links are repaired differently [84]. Replication protein A (RPA) has been shown to recognize interstrand cross-links caused by the platinum-based chemotherapy drug cisplatin [85]. Phosphorylation of *FANCM* recruits the rest of the FA core complex to chromatin [86]. The FA core complex is composed of *FANCA*, *FANCB*, *FANCC*, *FANCE*, *FANCF*, *FANCG*, *FANCL*, and *FANCM* and promotes monoubiquitination of the ID2 complex [86]. Monoubiquitination of the ID2 complex, composed of *FANCI* and *FANCD2*, activates the complex. The exact function of the ID2 complex has not been fully elucidated. XPF and ERCC1 are both involved in ICL to fix cross-link-induced double-strand breaks through "unhooking" (chemical cleavage) of the cross-link [87–89]. This event depends on ubiquitination of FANCD2 and interaction with SLX4 (FANCP) [89]. Protein

encoded by the HDR genes, including breast/ovarian cancer susceptibility genes *BRCA1*, *BRCA2*, *BRIP1*, *PALB2*, *RAD51C*, and *XRCC2* are all involved in ICL to fix DSBs and are recessive FA genes [52,78,90–93].

A 2.5-year-old Saudi child presented with a case of FA but did not have a mutation in any of the known FA genes [51]. Whole-exome sequencing identified a homozygous nonsense mutation (p.Arg215*) in *XRCC2* [51]. In 2016, further research showed that *XRCC2* could complement the cellular defects in this patient's fibroblasts that are hallmarks of FA cells, namely hypersensitivity to DNA interstrand crosslinking agents, overabundance of cells in G2-M phase of the cell cycle, and chromosome breakage, illustrating that the *XRCC2* mutation is the causative mutation in this patient [52].

Development of assays for determining pathogenicity of missense substitutions in DSB repair genes

Effectively determining pathogenicity of unclassified missense substitutions is essential for clinical mutation screening. There are two types of variants of uncertain significance (VUS): variants that are unclassified and variants that are uncertain. Unclassified variants are sequence variants that have not previously undergone evaluation for pathogenicity. Uncertain variants are sequence variants that either do not have enough evidence to classify as pathogenic or neutral or have contradicting evidence for or against pathogenicity. With more mutation screening being performed via panel testing, the possibility of finding a VUS increases. Our lab's data suggest that for the breast cancer susceptibility genes *RAD50* and *XRCC2,* roughly 50% of the genetic risk attributable to these genes is caused by rare missense substitutions [94–

[96]. This presents significant challenges to screening patients in the clinic. In an attempt to determine the pathogenicity of VUS in intermediate-risk breast cancer susceptibility genes, we planned to develop a functional assay to test different mutations found previously by the lab during case-control mutation screening of human breast cancer patients [94–97]. To attempt to develop a system to assay variants in *RAD50* and *XRCC2*, we planned to use zebrafish as our model organism.

Zebrafish model

While the sequence analysis and family study-based components of missense substitution evaluation that were developed for *BRCA1* and *BRCA2* also apply to *RAD50* and *XRCC2*, we believe that medium throughput functional assays will play a critical role to decrease the number of VUS in these two genes [98–101]. Many of the key DNA double-strand break repair genes are conserved in zebrafish [102,103]. Zebrafish offer a unique model because null mutations in genes including *brca2*, which would be lethal in mammals, are tolerated in zebrafish [104–106]. The other benefit of using zebrafish is the power of embryo injection assays, allowing mRNAs containing sequence variants of interest to be injected into mutant zebrafish.

Results from the embryo injection functional assays can be combined with *in silico* predictions and patient family history to perform an integrated evaluation of each missense substitution [98–101]. Functional assays have already been conducted on some *CHEK2* sequence variants [23,107]. RNA injection experiments are beginning to be performed in zebrafish to assess the pathogenicity of rare missense substitutions in *kcnh2* and *hcn4*, genes involved in Long QT syndrome and Sick Sinus Syndrome, respectively

[108,109]. Methods exist for rapid generation of many mRNAs containing the missense substitutions of interest using the methods described in Drost *et al*., 2010 [110]. As radiosensitivity is a phenotype for both *RAD50* and *XRCC2*, we planned to assay cleaved Caspase-3 via whole-mount immunofluorescence and perform western blots for γH2AX following irradiation [111,112]. Both genes are involved in DNA DSB repair, so we also planned to utilize a damaged GFP assay to quantify changes in HDR [113].

To develop lines to assay our human sequence variants, we first needed to generate null mutations in the zebrafish copies of *rad50* and *xrcc2*. We used transcription activator-like effector nucleases (TALENs) to create mutations in these genes. TALENs function by creating a double-strand break at a specific sequence [114]. If this break is repaired by NHEJ, then there is the possibility of creating a frameshift mutation [114]. For *rad50*, a 7 base-pair (bp) frameshift mutation was recovered in exon 3, disrupting the ATPase-N domain, also resulting in a premature stop codon. Deletions of 8 and 10 bp were generated in *xrcc2* in the third and final exon in *xrcc2*, disrupting most of the P-loop NTPase domain. Each of these mutations was eventually characterized.

Because of the mutant phenotypes associated with *rad50* and *xrcc2*, we were unable to assay variants in either gene. However, these zebrafish mutations turned out to be the only existing vertebrate models of null mutations in either gene. As no research had been conducted on zebrafish *rad50* and *xrcc2*, we chose to characterize their mutant phenotypes.

CHAPTER 2

XRCC2 MUTATION IN ZEBRAFISH LEADS TO ABERRANT GONAD FUNCTION INCLUDING SEMINOMAS

Abstract

The DNA homologous recombination repair gene XRCC2 is one of 21 different genes associated with the disease Fanconi anemia (FA). Because of embryonic lethality in mammals, there is a lack of XRCC2 vertebrate models to study the effects XRCC2 has on development and tumorigenesis. To investigate the biological impact of XRCC2 on vertebrates, a zebrafish xrcc2 knockout was generated. All xrcc2-/- zebrafish develop exclusively as males due to female-to-male sex reversal, a pattern consistent with other zebrafish FA gene mutants. xrcc2 is expressed at significantly higher levels in the gonads than in other tissues. The male sex skew was rescued by introducing the tp53(M214K) allele, which allowed tp53(M214K/M214K);xrcc2-/- females to develop. Testicular neoplasias, specifically seminomas, developed in the xrcc2-/- males beginning around roughly 20 months of age, indicating tumor suppressor function of xrcc2 in male gonad. By rescuing the sex skew of xrcc2 and analyzing tumors, we support the findings that XRCC2 is an FA gene and that FA genes play a key role in germ cell biology.

Author summary

XRCC2 is an important DNA repair gene and has been associated with Fanconi anemia (FA). However, because of embryonic lethality in mammals, few developmental models exist to study *XRCC2* function. Because of this, little is known about the role *XRCC2* plays in later vertebrate development. Using zebrafish, we report the first viable vertebrate model with an *XRCC2* mutation. *xrcc2* mutant zebrafish exhibit the hallmarks of FA gene mutants in zebrafish including female-to-male sex reversal, with all fish developing into fertile males. This male sex skew can be rescued by mutation of *tp53* using the dominant-negative hypomorphic *zdf1* (p.Met214Lys) allele, which allows for fertile, double mutant females to develop. *xrcc2* is highly expressed in the gonads of wild-type zebrafish. The *xrcc2* mutant zebrafish showed 3-fold decreased expression ($p<0.05$) of *amh* in their testes and 1.2-fold testicular expression ($p=0.20$) of *dmrt1a* and 1.5-fold increased expression ($p=0.21$) of *igf3*. Testicular germ cell tumors also develop in the xrcc2 mutants, with approximately 30% incidence by age 23 months.

Introduction

XRCC2 (*X-ray repair cross complementing gene-2*, [OMIM 600375]) is a DNA homologous-recombination-repair gene as well as a strong candidate moderate risk breast cancer susceptibility gene [95]. *XRCC2* is one of the five paralogs of the *Escherichia coli RecA* homolog *RAD51* and was discovered and cloned based on its ability to rescue the DNA damage repair defect in the irs1 Chinese hamster cell line [43]. The five *RAD51* paralogs, *RAD51B*, *RAD51C*, *RAD51D*, *XRCC3*, as well as *XRCC2*, are necessary for the repair of DNA double-strand breaks by homologous recombination [115]. *XRCC2* shows

protein sequence conservation from humans to *Trichoplax adhaerens* [95]. While several studies have failed to replicate the finding of *XRCC2* as a breast cancer susceptibility gene [116–118], *XRCC2* has been shown to interact with the products of breast and/or ovarian cancer susceptibility genes *RAD51B*, *RAD51C*, and *RAD51D* as part of the BCDX2 complex, which is necessary for the formation of *RAD51* foci [44–49]. Biallelic mutations in *RAD51C* and *XRCC2* have been shown to cause Fanconi anemia [52,79,80,93].

Fanconi anemia (OMIM 227650) is a rare genetic disease caused by 21 different genes involved in interstrand crosslinking (ICL) repair and the interface between ICL repair and the homologous recombination repair (HRR) pathway [52,78–82]. Several known breast and/or ovarian cancer susceptibility genes are also recessive FA genes (e.g., *BRCA1*, *BRCA2*, *BRIP1*, *PALB2*, and *RAD51C*) [78,90–93]. Symptoms of FA include bone marrow failure, congenital defects, chromosomal instability, hypersensitivity to DNA crosslinking agents, and cancer predisposition, including acute myeloid leukemia and squamous cell carcinoma of the head and neck [82,119,120]. In a previously unexplained case of FA in a 2.5-year-old Saudi child, whole exome sequencing was conducted, and a homozygous nonsense mutation (p.Arg215*) in *XRCC2* was identified as the likely cause [51]. It was further shown that three hallmarks of FA cells (hypersensitivity to interstrand crosslinking agents, chromosome breakage, and accumulation of cells in G2-M during the cell cycle) could all be rescued in primary fibroblasts from that patient by complementing with wild-type *XRCC2* [52]. These findings led to the designation of *XRCC2* as an FA-like gene, *FANCU* [52]. Mutations in FA genes have also been shown to result in defects in germ cell development and sex determination [104,121–125].

While having two different sexes is common in animal species, sex determination

is achieved in a variety of different ways. Some vertebrate species rely on sex chromosomes or other genetic factors to determine sex. Others use environmental factors such as temperature for sex determination, and some species use a combination of both. For example, medaka (*Oryzias latipes*) has XX/XY sex determination but XX females can develop into males at high temperatures [126]. Despite being a commonly used model organism, the sex determination mechanism in zebrafish (*Danio rerio*) has not been fully elucidated. While there are no obvious sex chromosomes in zebrafish [127–129], sex determination in zebrafish is primarily due to genetic as opposed to environmental factors (reviewed in Liew and Orbán [130]). Loss of germ cells, either through ablation or mutation of genes including *dead end* and *nanos3*, leads to the development of sterile males to the exclusion of females; this finding illustrates the requirement of viable oocytes for female development in zebrafish and does not appear to depend upon the oogonial stem cells [131–134]. Additionally, inhibition of aromatase results in the female-to-male sex reversal of adult zebrafish [135].

The FA/BRCA gene network, which is largely intact in zebrafish, has proven to be important in zebrafish sex determination [136]. To date, FA genes *brca2* (*fancd1*), *fancl*, and *rad51* have been mutated in zebrafish [104,121,125]. All show female-to-male sex reversal in homozygous mutants [104,105,121,125] (and reviewed in Rodríguez-Marí and Postlethwait [137]). Both *brca2* and *fancl* are expressed in the gonads of wild-type zebrafish, with *brca2* and *fancl* mutants showing increased germ cell apoptosis [105,121]. The *tp53* mutant allele *zdf1* (p.Met214Lys), which is a dominant-negative hypomorphic allele, complements the *brca2*, *fancl*, and *rad51* developmental defect, decreasing germ cell apoptosis and rescuing the male sex skew [104,105,121,125,138,139]. Testicular neoplasias,

including seminomas and papillary cystadenomas, have been observed in *brca2* mutants [104,105].

Results

xrcc2-mutant zebrafish are all fertile males due to female-to-male sex reversal

To investigate the role of *xrcc2* in zebrafish development and tumorigenesis, a transcription activator-like effector nuclease (TALEN) was used to induce a frameshift mutation early in exon 3 of *xrcc2*, disrupting most of the P-loop NTPase domain. Two different frameshifted alleles were generated, an 8-base-pair (bp) and a 10-bp deletion (Fig. 2.1A). The *xrcc2* 8-bp and 10-bp alleles were genotyped by high-resolution melting (HRM) curve analysis (Fig. 2.1B and 2.1C). *xrcc2* heterozygotes were incrossed to generate *xrcc2* homozygotes. From 131 incrossed fish, 34 were *xrcc2* homozygotes, all of which were male. In contrast, the sex ratios were normal for wild-type and heterozygous fish (Fig. 2.2A). There are two possible explanations for this: female lethality or female-to-male sex reversal as seen in *brca2*, *fancl*, and *rad51* [104,121,125]. To deduce which was occurring, *xrcc2* homozygote males were crossed to *xrcc2* heterozygote females. For this cross, the number of homozygotes should be equal to heterozygotes; however, if the number of homozygotes is significantly smaller, it would indicate female lethality. In the cross, we recovered 112 *xrcc2* homozygotes, which were again all male, and 108 (77 females and 31 males) heterozygotes (Fig. 2.2B). This finding indicated that the male sex skew in the *xrcc2* homozygotes is due to female-to-male sex reversal and not female lethality.

xrcc2 is predominantly expressed in the gonads of wild-type zebrafish and aberrant gene expression occurs in _xrcc2_-mutant testes

Given the female-to-male sex skew in *xrcc2* homozygotes, *xrcc2* expression was compared between wild-type and *xrcc2*$^{-/-}$ adult flank (posterior of the anal fin), gut, head (anterior of the gill slit), and testis tissue. *xrcc2* mRNA was also measured in wild-type ovaries. The frameshift mutation is contained within the third and final exon of *xrcc2*. Nonsense mediated decay (NMD) has been known to be inefficient when the premature stop codon is located downstream of the last exon junction complex (EJC) [140]. To determine *xrcc2* expression, quantitative reverse transcription PCR (qRT-PCR) was conducted for *xrcc2*; *β-actin* was used as the loading control [141]. *xrcc2* was expressed 98-fold higher ($p<0.05$) in wild-type testis and 75-fold higher ($p<0.05$) in ovary tissue compared to the flank, gut, and head (Fig. 2.3A).

There was no significant difference ($p>0.05$) in *xrcc2* expression between the wild-type flank, gut, or head, and the homozygous mutant flank, gut, or head, indicating that the *xrcc2* mRNA does not appear to be degraded by NMD in *xrcc2* homozygotes. Expression of *xrcc2* in the homozygous mutant testes was 3-fold lower ($p<0.05$) than in the wild-type testes. All the *xrcc2* transcript from the mutants showed the frameshift deletion mutation as detected by HRMA (data not shown).

Anti-Müllerian hormone (*amh*) is produced in zebrafish Sertoli cells and is a marker of males [142]. We used qRT-PCR to compare *amh* expression in wild-type and *xrcc2*$^{-/-}$ testes and wild-type ovaries. Wild-type testes had 3-fold higher expression ($p<0.05$) of *amh* than the *xrcc2*$^{-/-}$ testes and 64-fold higher expression ($p<0.05$) than wild-type ovaries (Fig. 2.3B). The *xrcc2* testes had 20-fold higher expression ($p<0.05$) of *amh*

than the wild-type ovaries. We also examined expression of other genes involved in sex determination, including *doublesex and mab-3 related transcription factor 1a* (*dmrt1a*) and *insulin-like growth factor 3* (*igf3*), both of which are important in male germ cell biology [143,144]. While neither of these genes were significantly different between wild-type testis and *xrcc2*-mutant testis, *igf3* had 1.5-fold elevated expression (p=0.21) in the *xrcc2*-mutant testis compared to wild-type (Fig. 2.3C), while *dmrt1a* expression was decreased 1.2-fold (p=0.20) in the *xrcc2*-mutant testis compared to wild type (Fig. 2.3D).

Mutating *tp53* rescues male sex skew in *xrcc2* mutants

Previous studies on FA mutants in zebrafish reported that only a $tp53^{zdf1/zdf1}$ background rescued the female-to-male sex skew, allowing for development of viable double-homozygote females. *xrcc2* mutants were crossed into a $tp53^{zdf1}$ background. The $tp53^{+/zdf1}$;$xrcc2^{+/-}$ fish were incrossed, and the offspring were genotyped. We observed *tp53* rescue in the *xrcc2* mutants, generating 13 double-homozygote females (Fig. 2.4). To recover these 13 double homozygote females, $tp53^{zdf1/zdf1}$;$xrcc2^{+/-}$ fish were incrossed (Fig. 2.4). The $xrcc2^{-/-}$ genotype did not have a notably different male-to-female sex ratio compared to $xrcc2^{+/+}$ or $xrcc2^{+/-}$ in the $tp53^{zdf1/zdf1}$ background (Fig. 2.4).

Testicular germ cell tumors were observed in *xrcc2* mutants

As previously reported, *brca2* mutant zebrafish develop testicular neoplasia, originating from somatic and germ cells [104]. Because of this, *xrcc2* mutants were monitored for tumor development. From 20-22.5 months (mo) of age, the *xrcc2* mutants developed seminomas (Fig. 2.5A). Eight out of 26 (30.8%) *xrcc2* mutants developed

tumors by age 22.5 mo. Seven out of 8 tumors were seminomas. The other tumor was a disseminated round cell tumor, histologically most consistent with a lymphoma and present in tissues including the eye, gill, gut, gut mucosa, kidney, and liver (Fig. 2.5B). One seminoma was observed among 6 age-matched wild-type controls, and no seminomas were observed among the 4 age-matched *xrcc2*$^{+/-}$ controls.

Mutant male gonads do not display other histologic changes

Gonad histology was examined for a total of 6 wild-type, 4 *xrcc2*$^{+/-}$, and 16 *xrcc*$^{-/-}$ male zebrafish. As previously mentioned, 6 of the *xrcc2*$^{-/-}$ and 1 wild-type male zebrafish had seminomas (Fig. 2.5B). All 4 of the *xrcc2*$^{+/-}$ had normal spermatogenesis and orderly maturation (data not shown). Of the 5 wild types that did not have a seminoma, 3 had normal spermatogenesis with orderly maturation (Fig. 2.6A). Two of the wild types had complete spermatogenesis with orderly maturation but possessed at least one small area of relatively increased spermatogonia (data not shown). This small area of increased spermatogonia was also observed in 2 of the 10 *xrcc2*$^{-/-}$ males (data not shown). One of the *xrcc2*$^{-/-}$ males showed testicular hypoplasia with arrested spermatogenesis (data not shown). The remaining 7 *xrcc2*$^{-/-}$ males had normal spermatogenesis with orderly maturation (Fig. 2.6B). Other than a relative increase in the incidence of seminoma in *xrcc2*$^{-/-}$ male zebrafish compared to *xrcc2*$^{+/-}$ and wild-type male zebrafish, there was no obvious and consistent difference in histomorphology of the testes between these groups.

tp53zdf1/zdf1;xrcc2-/- females have normal oogenesis but defects in the liver

The *tp53*-rescued *xrcc2*$^{-/-}$ females that do not possess tumors show complete oogenesis with orderly maturation of the oocytes (Fig. 2.7A). The *tp53*$^{zdf1/zdf1}$;*xrcc2*$^{-/-}$ females showed variable degrees of hepatocellular karyomegaly and binucleation (Fig. 2.7B). Of the 8 double-mutant females examined for histology, three had developed tumors (Fig. 2.7C and 2.7D). Two of the tumors were spindle cell sarcomas, which are frequently observed in *tp53*-mutant zebrafish (Fig. 2.7C). The third tumor was a hepatocellular carcinoma (HCC), a tumor not usually associated with *tp53*-mutation alone in zebrafish (Fig. 2.7D).

Discussion

We describe here the first viable vertebrate model of *xrcc2* mutation. *XRCC2* was first discovered and cloned due to its ability to complement the DNA-repair defects seen in the *irs1* Chinese hamster ovary (CHO) cell line, which has a point mutation causing aberrant splicing of the first intron [145–147]. Study of *XRCC2* has remained limited by the lack of a vertebrate model; for example, mouse *xrcc2*-mutants are perinatal lethal due to failed neurogenesis [148].

Zebrafish model supports _xrcc2_ as a Fanconi anemia gene

All of the current evidence that *XRCC2* is an FA gene comes from one human patient, who was homozygous for a p.Arg215* nonsense variant [51,52]. In this Saudi Arabian patient, complementation with *XRCC2* rescued the cellular defects characteristic

of FA cells, namely chromosome breakage, hypersensitivity to the interstrand crosslinking agent mitomycin C, and accumulation of cells in G2-M during the cell cycle [51]. These findings indicate the nonsense mutation in *XRCC2* was the causative mutation in this patient [52].

Three FA genes have been mutated in zebrafish: *brca2*, *fancl*, and *rad51* resulting in mutant zebrafish that develop as males only [104,121,125]. Zebrafish sex determination is not as simple as the system used in mammals; it appears to be driven by genetic factors despite the lack sex chromosomes [127–129] (reviewed in Liew and Orbán [130]). Oocytes appear to be required to maintain a female phenotype, and loss of oocytes, even in adult zebrafish, leads to female-to-male sex reversal [132–134]. Rodriguez-Marí et al. [121] found in *fancl* mutants that there was increased germ cell apoptosis due to failure of oocytes to progress through meiosis. A homozygous dominant-negative hypomorphic *tp53*^{M214K} background decreased germ cell apoptosis rescued the male sex skew seen in *brca2*, *fancl*, and *rad51* homozygotes [104,105,121,138,139]. *Fance* mutant mice show both primary ovarian insufficiency and delayed testicular germ cell maturation [122,149]. Similar to zebrafish, *Fanca*$^{-/-}$; *Fancg*$^{-/-}$ double-mutant mice display defects in the ovaries with hyperplasia of interstitial cells and decreased follicle development [150].

The *xrcc2* mutants display a male sex skew caused by female-to-male sex reversal, which is consistent with results from *brca2*, *fancl*, and *rad51* mutants [104,121,125]. Also consistent with the other FA gene mutants, complementing *xrcc2* with *tp53*^{M214K} rescued the sex skew, and allowed us to recover viable, fertile females. The *xrcc2* mutant males developed seminomas at a frequency of 30.8% at 20-22.5 mo, which is consistent with the findings for the *brca2* mutant [104].

Gene expression in the gonads of wild-type and *xrcc2*-mutant zebrafish

Because of the sex determination defect in *xrcc2* mutants, we compared expression of several different genes, including *xrcc2* and genes important for sex determination, in the gonads along with flank, gut, and head of wild-type and *xrcc2* mutants. We found that *xrcc2* is expressed at notably higher levels in testis and ovary than in other tissues in wild-type zebrafish. This result, along with the sex skew, points towards an important role for *xrcc2* in germ cell biology.

In zebrafish, *amh* shows differential expression that is indicative of males, is restricted to the gonads, and is produced primarily by Sertoli cells [148,151,152]. In mammals, *AMH* represses formation of Muëllerian ducts in males, and it is involved in preventing primary ovarian insufficiency [68,153,154]. The function of *amh* differs slightly in zebrafish versus mammals because teleost fish lack Müllerian ducts [142,155,156]. We found that wild-type testis had the highest *amh* expression, and wild-type ovaries had the lowest of the tissues examined. The *xrcc2* mutant testis fell in the middle, with significantly higher expression than the wild-type ovary and significantly lower expression than wild-type testis. Female FA patients have been shown to exhibit less AMH in their serum, which may help explain the primary ovarian insufficiency often seen in these patients [68]. Fanc mRNAs may be enriched in mouse Sertoli cells, with FANCB, FANCM, and FANCI localizing to the nucleus and/or cytoplasm of Sertoli cells in mice [157].

The zebrafish *dmrt1* gene has three alternatively spliced isoforms, encoding proteins with varying lengths of 267, 246, or 132 amino acids, denoted a, b, and c respectively [143]. *Dmrt1a* is expressed at higher levels than the b and c isoforms [143]. *dmrt1* shows differential expression between males and females in the black porgy

(*Acanthopagrus schlegeli*) fish species, with expression localized to Sertoli cells during development [158]. Expression of *dmrt1* in Sertoli cells has also been reported in medaka, tilapia, and playfish [159–161]. In mice, *Dmrt1* is required for testis differentiation and is expressed in Sertoli and germ cells [162]. Sertoli cell function is lost in *Dmrt1*$^{-/-}$ mice [162].

Given the low levels of *amh* and moderate decrease in *dmrt1a* expression in *xrcc2*$^{-/-}$ testes, we hypothesized that there was a decrease in the number or function of Sertoli cells in *xrcc2*$^{-/-}$ fish. We therefore decided to examine another Sertoli cell marker, *igf3* [144,163]. *igf3* is expressed highly in the gonads with lower expression in other tissues like gills, and the *igf3* gene is only present in teleost fish [163–165]. Given our hypothesis, we expected to find decreased *igf3* expression in *xrcc2*$^{-/-}$ testis compared to wild type. Instead, we found that *igf3* was moderately elevated in *xrcc2*$^{-/-}$ testes compared to wild type. Indeed, Nóbrega et al. [163] reported that follicle-stimulating hormone (Fsh) promotes spermatogenesis through up-regulation of *igf3* and repression of *amh* in zebrafish. Moreover, elevated FSH levels have been observed in FA patients [70]. The histologic findings did not show any defect in the number of Sertoli cells but also did not show consistent differences in spermatogenesis in the *xrcc2*$^{-/-}$ male zebrafish.

These expression changes may play a role in the tumorigenesis that was observed in *xrcc2* mutant testes. In patients with seminomas, serum FSH levels were found to negatively correlate with spermatogenesis [166]. Elevated FSH levels were also found in seminoma patients compared to controls and nonseminoma germ cell tumors [167]. In humans, it is known that *IGF*s have antiapoptotic properties [168]. Additionally, IGFBPs, negative regulators of IGF signaling, are downregulated in seminomas [169]. Since it was only discovered in 2008, little is known about *igf3*, so further study is needed to elucidate

the functional consequence of potentially elevated *igf3* in *xrcc2*-mutant testis and if it contributes to the development of seminomas in these fish.

The male sex skew is rescued by a *tp53* mutation

For the other known zebrafish FA gene mutants, crossing in the *tp53 zdf1* allele, a missense substitution in the DNA binding domain, rescues the female-to-male sex skew [104,105,121]. Despite the *zdf1* allele being dominant negative, previous studies found that only $tp53^{zdf1/zdf1}$ could rescue the male sex skew [104,105,121]. For *xrcc2*, we found that the *tp53*-mutant background was sufficient to rescue $xrcc2^{-/-}$ females. Since crossing the *xrcc2* mutation into the *tp53*-mutant background rescues the sex skew in the *xrcc2* mutants, this finding illustrates that the mechanism for the sex switch in the *xrcc2* mutants is the same as in the *brca2*, *fancl*, and *rad51* mutants.

***xrcc2* mutants develop testicular germ cell tumors**

In *xrcc2* mutants, testicular germ cell tumors (TGCTs), all of which were seminomas, were observed beginning at roughly 20 months of age. Human TGCTs have a 10-year survival rate of nearly 95% [170]. Standard treatment often involves platinum-based chemotherapy agents (e.g., cisplatin), which is effective for most cases [170–172]. Roughly 3% of tumors are cisplatin-refractory [172]. Patients with treatment-refractory tumors have a poor prognosis [173]. Litchfield et al. [172] reported whole exome sequencing from 2 treatment-refractory TGCTs and 41 nonresistant TGCTs. *xrcc2* mutations were present in both of the treatment-refractory TGCTs and none of the nonresistant TGCTs [172]. A naturally occurring variant in *XRCC2* (R188H) confers cisplatin-resistant in

humans [174]. Testicular neoplasia, including both germ cell and somatic cell tumors, were also observed in the *brca2* mutant zebrafish [104]. In this paper, we present the first seminoma model that is mutant for *xrcc2*.

Gonad and germ cell development is normal prior to tumorigenesis in males

Despite promising qRT-PCR results, no consistent histologic differences were observed in the male gonads of the *xrcc2* mutants compared to heterozygotes or wild types. We therefore cannot explain the qRT-PCR results based on differences in the number of Sertoli cells or differences in spermatogenesis.

Rescued female gonads and oocytes develop normally but there are liver abnormalities

In the $tp53^{zdf1/zdf1}$;$xrcc2^{-/-}$ females, oogenesis occurred normally, which is in contrast to $tp53^{zdf1/zdf1}$;$brca2^{Q658X/Q658X}$ females that showed binucleated oocytes [104]. Observation of 2 spindle cell sarcomas in the $tp53^{zdf1/zdf1}$;$xrcc2^{-/-}$ females is not a surprising finding given that this tumor type is common in *tp53*-mutant zebrafish [138]. However, HCC is not typically seen in *tp53*-mutant zebrafish lacking another mutation, but was observed when *myca* was overexpressed in the liver in a *tp53*-mutant background [175]. Overexpression of *HBx* or *src* in the liver of *tp53*-mutant zebrafish also drives HCC formation [176]. Hepatocellular karyomegaly and binucleation were observed in the double-mutant females. Traditionally, these liver phenotypes are thought to be related to toxicant exposure, but it has yet to be determined what the causative agent(s) is/are [177]. However, since hepatocellular karyomegaly and binucleation were not observed in any of

the other zebrafish, there is a possibility that the *tp53*$^{zdf1/zdf1}$; *xrcc2*$^{-/-}$ genotype contributes to the liver phenotypes. Whole-exome sequencing of a hepatitis C virus-positive HCC revealed the presence of a missense substitution in *XRCC2* (p.R91Q) [178]. Further research will be needed to determine what, if any, role *xrcc2* mutations play in HCC and other liver pathology observed in the *tp53*$^{zdf1/zdf1}$;*xrcc2*$^{-/-}$ females.

Materials and methods

Ethics statement

All animals used in this study were used in accordance with the policies of the University of Utah Institutional Animal Care and Use Committee following approved protocol 16-03003.

Animals

Zebrafish *xrcc2* mutations were generated through transcription activator-like effector nuclease (TALEN) mutagenesis [114]. The *xrcc2* TALEN recognition sequences were as follows: *xrcc2* TALEN L: ACCACCTAATCACCCGCT *xrcc2* TALEN R: CCAGACCTCCACTGT, and made by the Utah Mutation Generation and Detection core facility. The *tp53* mutant line used was the *tp53*^{zdf1} (amino acid change M214K) and was obtained from ZIRC (http://zebrafish.org/zirc/home/guide.php) [138]. Genotyping of *tp53* was carried out according to the protocol in [138]. Zebrafish were housed at the CZAR (Centralized Zebrafish Animal Resource) facility at the University of Utah.

Genotyping of *xrcc2* mutants

Genotyping of *xrcc2* mutants was carried out by polymerase chain reaction (PCR) and high-resolution melting curve analysis (HRMA) [179–181]. Genomic DNA was isolated by alkaline lysis (incubation in 20-40 µl of 50 mM NaOH at 95 °C for 20 minutes, followed by addition of 2-4 µl of 1M Tris pH 8.0). Added to the PCR reaction for HRMA was LCGreen Plus+ Melting Dye [BioFire Defense BCHM-ASY-0005]. PCR conditions were: 2' 95 °C; 42 cycles of 10" 95 °C, 15" 62 °C, 10" 72 °C; followed by 2' 95 °C then hold at 12 °C. The PCR product size is 102 bp for WT, 94 bp for the 8-bp deletion mutant, and 92 bp for the 10-bp deletion mutant. The completed PCR reaction was then analyzed by HRMA with a temperature range of 70 °C to 95 °C on a LightScanner HR I 96 [Idaho Technology Inc.] using small amplicon-based genotyping for melting curve data analysis.

RNA isolation and qRT-PCR

Dissected tissues were briefly washed in 1X phosphate buffered saline (PBS) pH 7.4 and placed in 600 µl of TRIzol® Reagent (Thermo Fisher Scientific 15596026). The following tissues were used: flank (posterior of the anal fin), gut, head (anterior of the gill slit), ovary, and testis. Tissues from four different fish were pooled for each sample. Tissues were homogenized using a Kontes Pellet Pestle Motor. Purified RNA was isolated using the Direct-zol™ RNA MiniPrep Plus (Zymo Research R2072) according to the manufacturer's protocol, including the DNase I treatment step. RNA concentration and quality was assessed using a NanoDrop, ND-1000 Spectrophotometer. 1 µg of DNase I-treated RNA was reverse transcribed with random hexamer primers to produce

cDNA using the SuperScript® III First-Strand Synthesis System (Thermo Fisher Scientific 18080051) according to the manufacturer's protocol. Quantitative reverse transcription PCR (qRT-PCR) was carried out using PowerUp™ SYBR™ Green Master Mix (Thermo Fisher Scientific A25742) for the following genes: *β-actin*, *amh*, *dmrt1a*, *igf3*, and *xrcc2* [141,164,182,183]. Expression was calculated using $2^{-\Delta\Delta CT}$ and normalized to *β-actin*.

Tumor isolation

Zebrafish aged 20-22.5-months post fertilization (mpf) were fixed in 4% paraformaldehyde (PFA) for one week at 4 °C. The fish were removed from the 4% PFA and washed twice in 1X PBS pH 7.4. The fish were then placed in 0.5M ethylenediaminetetraacetic acid (EDTA) pH 8.0 for one week at room temperature. Fish were then bisected along the sagittal plane. Research Histology at the Huntsman Cancer Institute (Salt Lake City, UT) performed paraffin embedding, para-sagittal sectioning with cut-side up, and stained with hematoxylin and eosin. Tumors were evaluated by two pathologists (HRS and KJE).

Gonad histology

The slides for gonad histology were prepared as described above for tumor isolation utilizing 20-22.5 mpf wild-type, *xrcc2*$^{+/-}$, and *xrcc2*$^{-/-}$ male zebrafish or 12 mpf *tp53*$^{zdf1/zdf1}$; *xrcc2*$^{-/-}$ females. Gonad histology was evaluated by a veterinary pathologist (HRS).

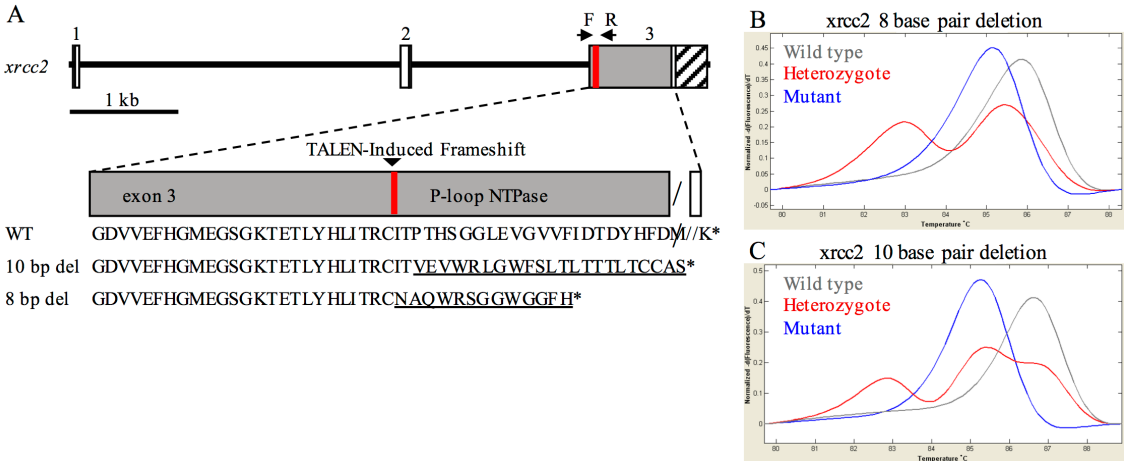

Figure 2.1. TALEN-induced frameshift mutation in zebrafish *xrcc2*. (A) Zebrafish *xrcc2* gene structure showing the TALEN cut site in the third and final exon. F and R indicate the forward and reverse primers for genotyping and qRT-PCR of *xrcc2*. Two xrcc2 mutant alleles were generated, an 8-base-pair (bp) and 10-bp deletion with the resulting amino acid changes that occur in each mutation in exon 3. Both result in a frameshift that disrupts most of the P-loop NTPase domain, without causing nonsense mediated decay. HRM genotyping curves of a wild-type, heterozygote, and homozygote for the *xrcc2* 8-bp (B) or 10-bp (C) deletion allele using the primers shown in (A).

Figure 2.2. *xrcc2* mutants are all male due to female-to-male sex reversal and not female lethality. (A) The bars represent the number of fish that are male (lines) or female (dots) for wild-type, heterozygote, and homozygote *xrcc2* genotypes. Within the *xrcc2*$^{-/-}$ genotype, only males are observed, while normal sex ratios were seen for wild types and heterozygotes. (B) The bars represent the number of fish that are male (lines) or female (dots) for wild type, heterozygote, and homozygote *xrcc2* genotypes, with solid grey bars representing expected numbers for each genotype and gender. For a homozygote crossed to a heterozygote, the expected number of heterozygous progeny equals the expected number of homozygous progeny. Because that is the case for *xrcc2* with 112 homozygous progeny to 108 heterozygous progeny, we conclude that all homozygotes are males due to female-to-male sex reversal and not female homozygote lethality.

A

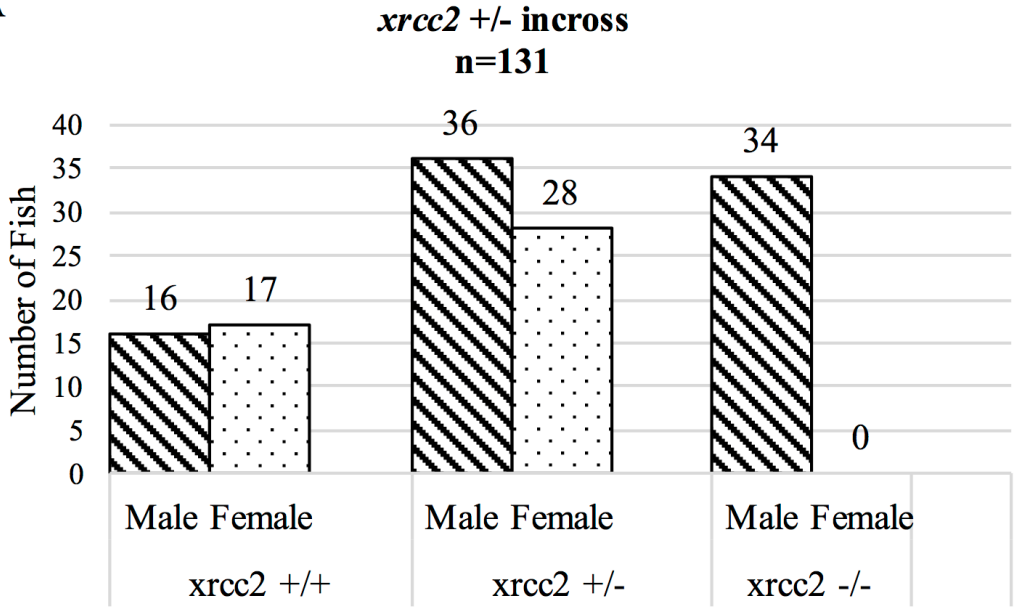
xrcc2 +/- incross
n=131
Number of Fish
40
35
30
25
20
15
10
5
0
16
17
36
28
34
0
Male Female
Male Female
Male Female
xrcc2 +/+
xrcc2 +/-
xrcc2 -/-

B

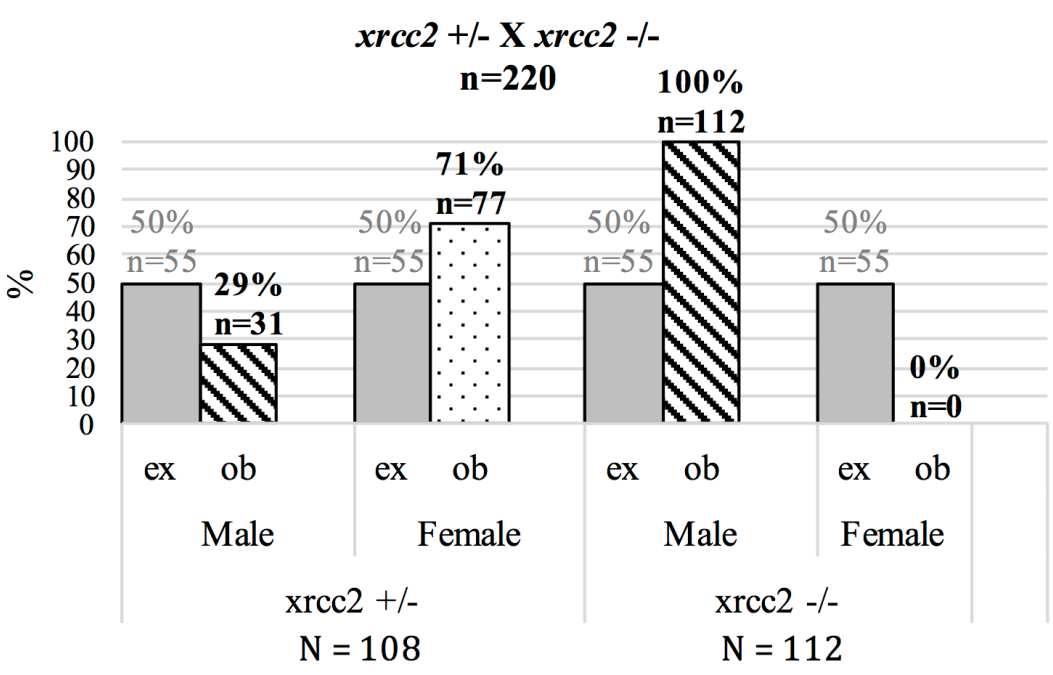
xrcc2 +/- X *xrcc2* -/-
n=220
%
100
90
80
70
60
50
40
30
20
10
0
50%
n=55
29%
n=31
50%
n=55
71%
n=77
50%
n=55
100%
n=112
50%
n=55
0%
n=0
ex ob
ex ob
ex ob
ex ob
Male
Female
Male
Female
xrcc2 +/-
N = 108
xrcc2 -/-
N = 112

Figure 2.3. *xrcc2*-mutant testes show aberrant gene expression compared to wild-type testes. (A) qRT-PCR expression of *xrcc2* in wild-type testis, ovary, flank (posterior of the anal fin), gut, head (anterior of the gill slit) and *xrcc2* mutant testis, flank, gut, and head. There was 98-fold higher expression ($p<0.05$) of *xrcc2* in wild-type testes and 75-fold higher expression ($p<0.05$) in wild-type ovaries compared to wild-type flank, gut, and head. Since the *xrcc2* mutation is in the final exon, the mRNA should not be subjected to nonsense mediated decay. There was no significant difference ($p>0.05$) in *xrcc2* expression in wild-type flank, gut, or head, and *xrcc2* flank, gut, or head, which suggests the transcript is not degraded. However, the *xrcc2* testes showed 3-fold less *xrcc2* expression ($p<0.05$) compared to wild-type testes. (B) *amh* is expressed 3-fold higher ($p<0.05$) in wild-type testis compared to *xrcc2* testis and 64-fold higher ($p<0.05$) than in wild-type ovaries. *amh* is expressed 20-fold higher ($p<0.05$) in *xrcc2* testis compared to wild-type ovaries. (C) 1.5-fold increased *igf3* expression in the *xrcc2*-mutant testes compared to wild-type testes is trending towards significance ($p=0.21$). *igf3* is expressed 4-fold higher ($p<0.05$) in *xrcc2*-mutant testes and 2.8-fold ($p=0.12$) in wild-type testes compared to wild-type ovaries. (D) 1.2-fold decreased *dmrt1a* in the *xrcc2* mutant testes compared to wild-type testes is trending towards significance ($p=0.20$). Wild-type testes had 508-fold higher expression ($p<0.05$) of *dmrt1a* than wild-type ovaries and *xrcc2*-mutant testes had 96-fold higher expression ($p<0.05$).

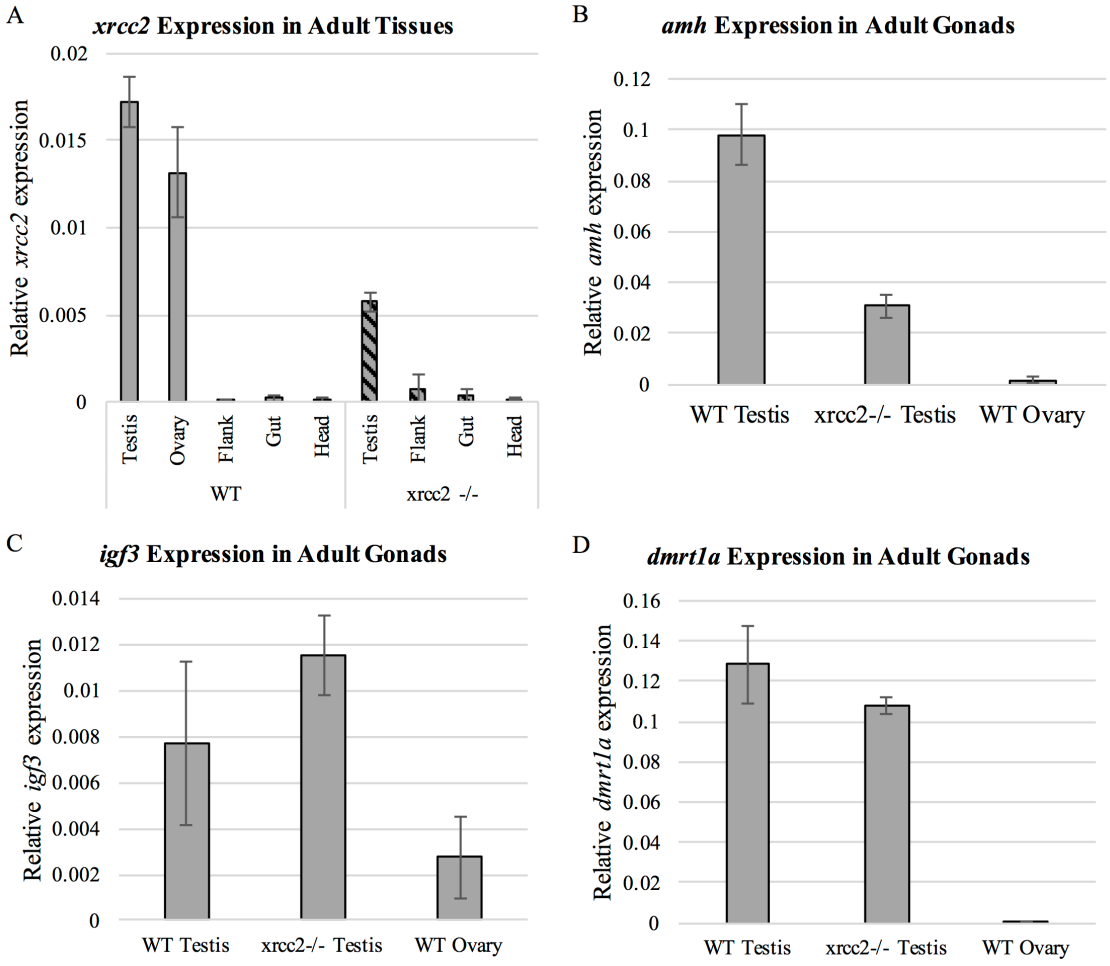
A
xrcc2 Expression in Adult Tissues
Relative xrcc2 expression
0.02
0.015
0.01
0.005
0
Testis
Ovary
Flank
Gut
Head
Testis
Flank
Gut
Head
WT
xrcc2 -/-
B
amh Expression in Adult Gonads
Relative amh expression
0.12
0.1
0.08
0.06
0.04
0.02
0
WT Testis
xrcc2-/- Testis
WT Ovary
C
igf3 Expression in Adult Gonads
Relative igf3 expression
0.014
0.012
0.01
0.008
0.006
0.004
0.002
0
WT Testis
xrcc2-/- Testis
WT Ovary
D
dmrt1a Expression in Adult Gonads
Relative dmrt1a expression
0.16
0.14
0.12
0.1
0.08
0.06
0.04
0.02
0
WT Testis
xrcc2-/- Testis
WT Ovary

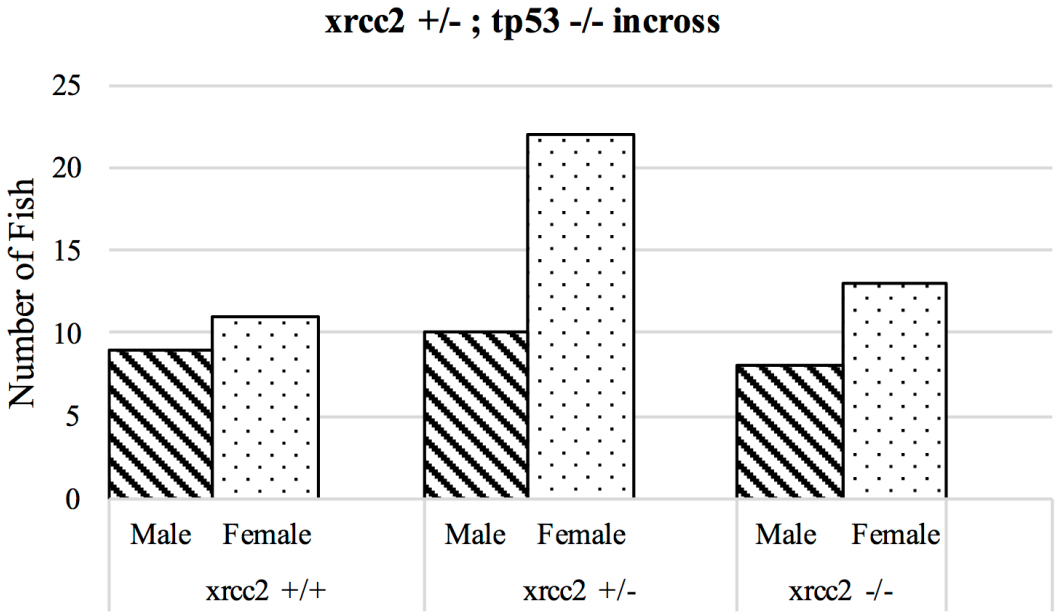

Figure 2.4. *tp53* mutations rescue the female-to-male sex reversal in *xrcc2* mutants. The bars represent the number of fish that are male (lines) or female (dots) for wild-type, heterozygote, and homozygote *xrcc2* genotypes in a *tp53*-mutant background. The mutant *tp53* allele used was *zdf1*, which is a dominant-negative missense substitution in the DNA binding domain.

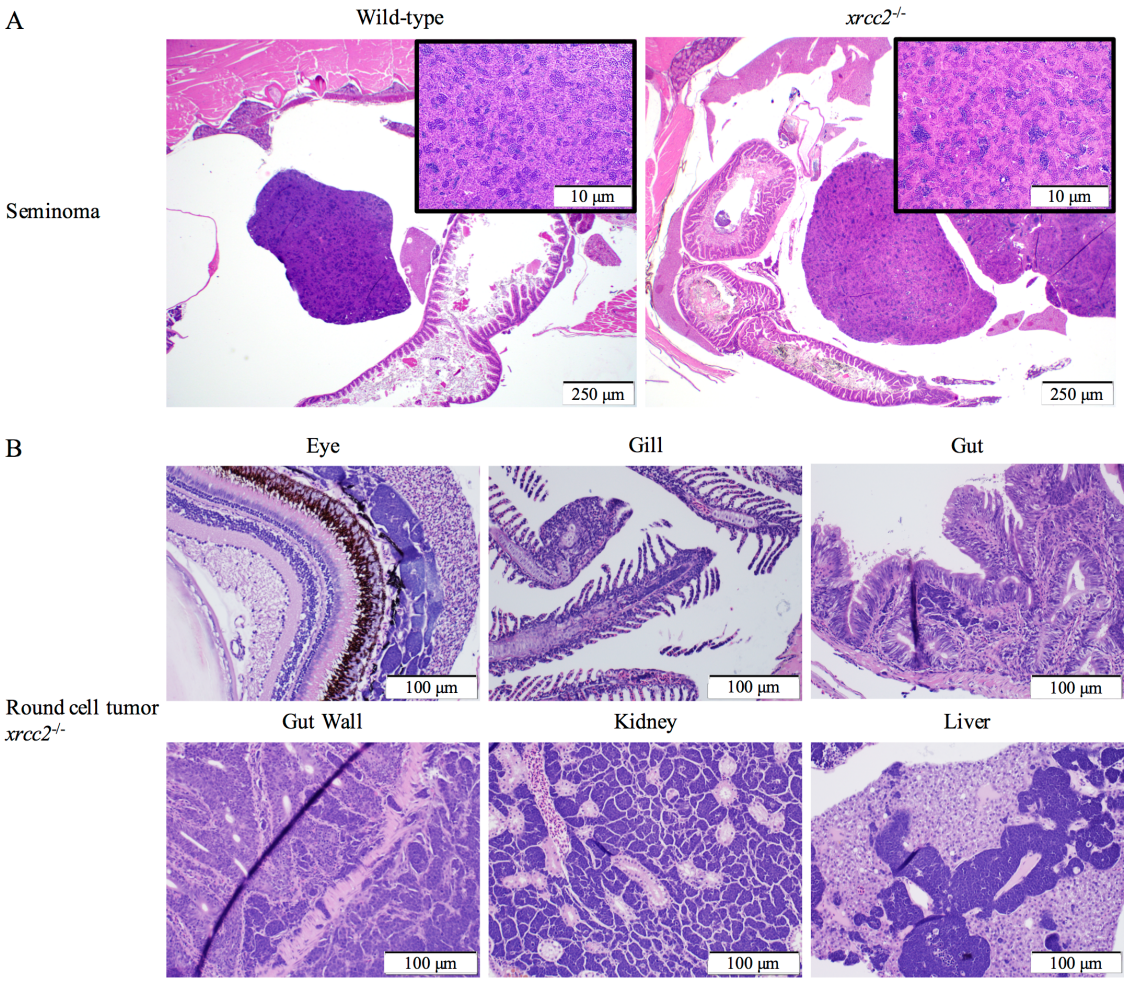

Figure 2.5. *xrcc2*-mutant males develop seminomas. At roughly 20 mo, *xrcc2* mutant males show seminomas. (A) Seminoma in an age-matched wild-type control and a representative seminoma from an *xrcc2* mutant male. (B) Disseminated round cell tumor, with morphologic features suggestive of lymphoma, present in the eye, gill, gut, gut wall, kidney, and liver in an *xrcc2* mutant male.

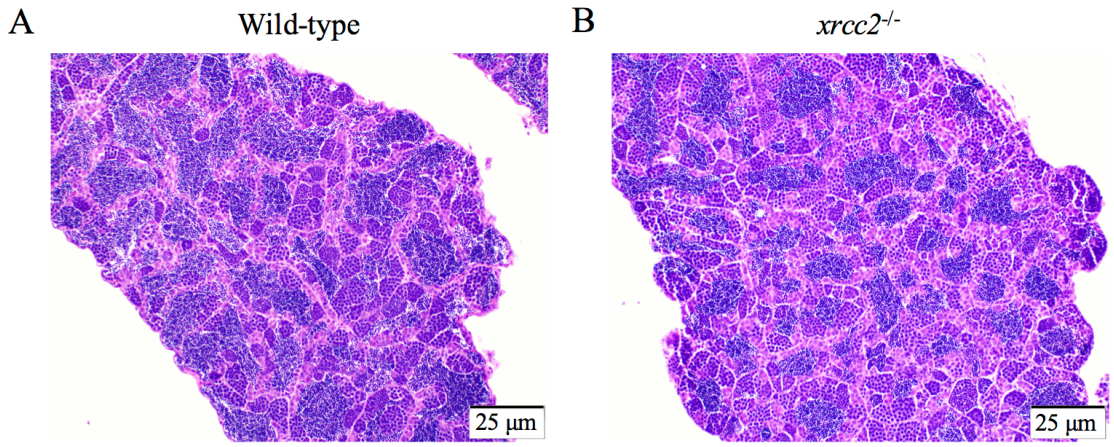

Figure 2.6. *xrcc2*-mutant male testes are histologically normal. Complete spermatogenesis with orderly maturation occurs in the majority of wild-type (A) and *xrcc2* mutant (B) males that are roughly 20 mo.

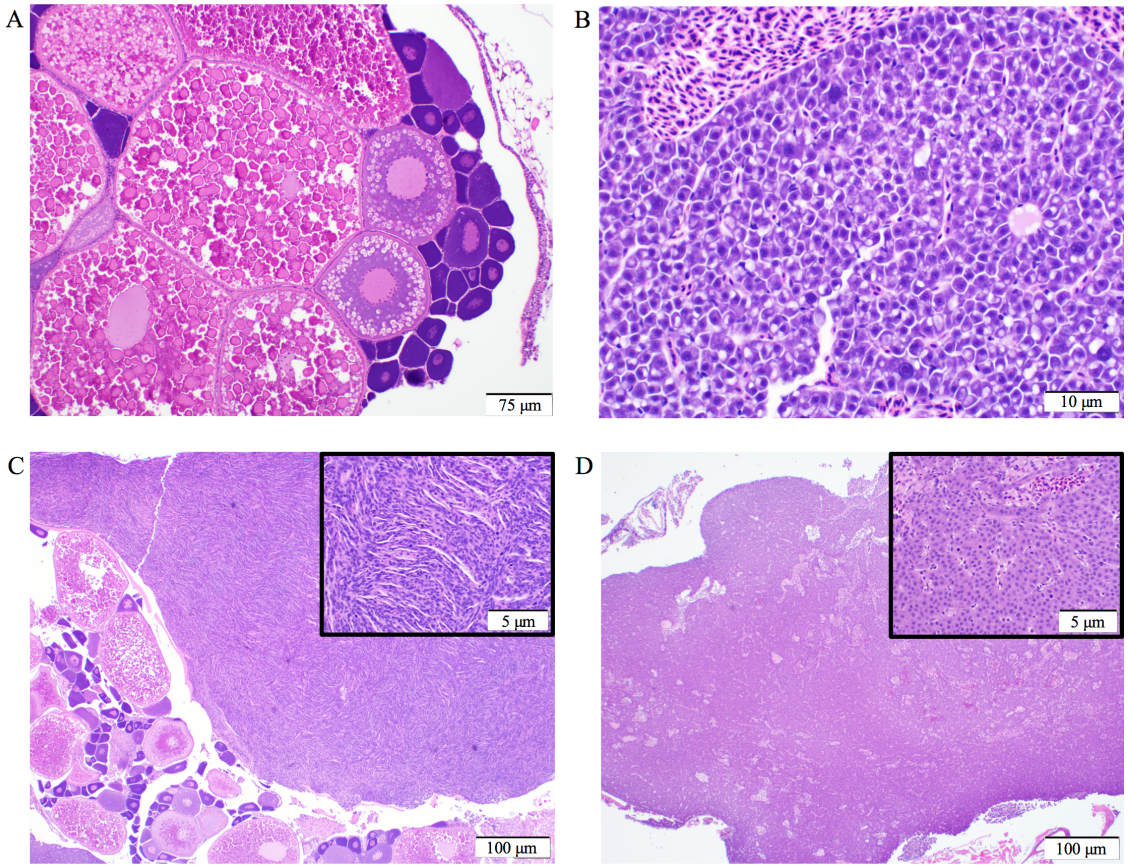

Figure 2.7. *tp53;xrcc2* double-mutant females have normal oogenesis but liver defects. **(A)** Complete oogenesis with orderly maturation of oocytes with all stages present occurs in the *tp53*$^{zdf1/zdf1}$;*xrcc2*$^{-/-}$ females. (B) Hepatocellular karyomegaly and binucleation present in the livers of *tp53*$^{zdf1/zdf1}$;*xrcc2*$^{-/-}$ females. (C) Spindle cell sarcoma in a *tp53*$^{zdf1/zdf1}$;*xrcc2*$^{-/-}$ female. (D) Hepatocellular carcinoma in a *tp53*$^{zdf1/zdf1}$;*xrcc2*$^{-/-}$ female.

CHAPTER 3

ZEBRAFISH *RAD50* MUTANTS HAVE A GROWTH DEFECT, HEMATOPOIETIC DEFECTS, AND RADIOSENSITIVITY

Abstract

RAD50 encodes a key protein in the DNA double-strand break (DSB) repair pathway, functioning in both the nonhomologous end-joining and homology-directed DSB repair pathways as part of the MRN complex with Mre11 and Nibrin. Biallelic mutation of *NBN* results in the disease Nijmegen breakage syndrome (NBS), and biallelic hypomorphic mutations in *RAD50* result in the clinically similar NBS-like disease. Because of its importance in early development, no vertebrate model for a null mutation in *RAD50* exists that allows for study in later development. We report here the first viable *rad50* null mutant using zebrafish. We found that *rad50*-mutant zebrafish share many clinical features with human NBS patients. These fish show decreased size, increased sensitivity to ionizing radiation, and hematopoietic defects.

Introduction

RAD50 encodes one of three proteins, along with *MRE11* and *NBN*, composing the MRN complex, which is a heterohexamer composed of dimers of each of these three proteins [184]. The MRN complex (called MRX complex in yeast) was first identified in a

screen for genes involved in DNA repair in *Saccharomyces cerevisiae* [185]. Each Rad50 protein binds an Mre11 protein and dimers of these form the "core" complex of the MRN complex [184]. Rad50, as part of the MRN complex, binds DNA using its N-terminal Walker A motif and C-terminal Walker B motif that bind each other to form an ATP-binding cassette (ABC)-type ATPase domain [14,186]. Nibrin functions to help with downstream signaling and proper localization of the MRN complex and interacts with the Rad50 flexible adapter [9,11,16–18]. The MRN complex associates with damaged DNA ends, playing a role in both DNA double-strand break repair and in recognizing exogenous viral DNA and limiting viral replication [184,187–190]. There are two main mechanisms for repair of DNA double-strand breaks (DSBs): nonhomologous end-joining (NHEJ) and homology-directed DSB repair (HDR) [3–5]. The MRN complex acts early enough in the DSB repair pathway that it promotes both NHEJ and HDR [191]. Like many DSB repair genes, all three genes in the MRN complex are either known or candidate moderate risk breast cancer susceptibility genes [96,192–194].

Ataxia-telangiectasia mutated (*ATM*) is an important downstream target of the MRN complex. ATM is a serine-threonine kinase that phosphorylates many different targets, including 53BP1, Chk1, Chk2, H2AX, KAP-1, p53, and SMC1 among others [195–201]. The MRN complex plays a role in ATM phosphorylation of targets Chk1, Chk2, and p53; however, there is no reduction in phosphorylation of histone H2AX with the loss of an MRN component [202–207]. Phosphorylated histone H2AX, which is called γH2AX, is an important signal for DNA damage repair [21,22]. In addition, ATM phosphorylates Nibrin, a step that is required for intra-S-phase checkpoint activation [208–211].

Biallelic loss-of-function mutations in *ATM* result in the disease ataxia-

telangiectasia (A-T) [71]. Patients carrying two *MRE11* mutations get the related disease ataxia-telangiectasia-like disorder (ATLD) [72]. Biallelic *NBN* mutations result in the disease Nijmegen breakage syndrome (NBS) [61,62]. While they are all distinct diseases, A-T, ATLD, and NBS all share some key features including cellular phenotypes and chromosomal abnormalities [61,73]. One main difference between A-T and NBS is that A-T patients suffer from cerebellar degeneration while this is not present in NBS patients [61,62,71,73]. While there are immunological deficiencies observed in A-T patients, they are due to errors in V(D)J recombination [212–214]. Hematopoietic failure is not observed in A-T patients, but it has been seen in NBS patients. A Japanese child with NBS presented with aplastic anemia, and two unrelated Russians with NBS presented with bone marrow aplasia in a study conducted on eight individuals [54,55]. One of the Russian patients also presented with acute myeloid leukemia (AML); coupling the finding of AML with the bone marrow failure illustrates key similarities of NBS to another disease caused by inherited mutations in DNA repair genes: Fanconi anemia [54]. Other clinical features of NBS include chromosomal instability, growth retardation, microcephaly, and radiosensitivity [61,62]. In addition to AML, non-Hodgkin lymphoma has been reported in children with NBS [215].

In 1991, a four-year-old German patient presented with symptoms consistent with NBS [75]. The patient did not carry two mutations in the *NBN* gene; however, the patient did carry two different mutations in *RAD50*, a nonsense mutation (c.3277C→T; p.R1093X) and a mutation that removed the stop codon (c.3939A→T) [50]. The loss of the stop codon mutation is predicted to add 66 additional amino acids (p.X1313YextX*66) and adds 5-10 kDa to the molecular weight of the Rad50 protein [50]. *RAD50* is highly

conserved at the C-terminus as determined from a protein multiple sequence alignment from humans through *Danio rerio*, illustrating why this mutation adding 66 amino acids is likely so damaging to Rad50 function [96]. This patient was found to have less than 5% of the Rad50 protein level compared to wild type [50]. Based on results from this human patient, biallelic *RAD50* mutations result in an NBS-like disease phenotype.

Rad50-null mice are not viable [74]. However, three different viable point mutations have been created in *Rad50* in mice; $Rad50^{S}$ (K22M), which is a point mutation in the Walker A motif, and two *Rad50* hook domain mutant, the $Rad50^{46}$ and $Rad50^{47}$ alleles, which are analogs to the yeast *rad50-46* and *rad50-47* alleles, which modify how the Zn^{2+} ion interacts with the Rad50 hook domain [76,77,216,217]. In the $Rad50^{S/S}$ mutants, the mice are decreased in size and die of hematopoietic failure beginning at 4-8 weeks of age [76,77]. These phenotypes can be rescued by mutating *p53*, but the double mutants then die instead of cancer faster than $p53^{-/-}$ alone from tumors that fall within $p53^{-/-}$ tumor spectrum [76,77,218].

Results

rad50 mutants are juvenile lethal and show a significant growth reduction

The role that *rad50* plays in zebrafish development was investigated through mutant generation using a transcription activator-like effector nuclease (TALEN). The TALEN was targeted to exon 3, disrupting the ATPase-N domain and creating a premature stop codon. A 7-base-pair (bp) frameshift mutation was recovered from the TALEN mutagenesis (Fig. 3.1A). Genotyping of the *rad50* 7-bp deletion was performed using high-resolution melting (HRM) curve analysis (Fig. 3.1B).

After the *rad50* mutants were generated with TALENs, the *rad50*$^{+/-}$ fish were incrossed to determine if the *rad50*$^{-/-}$ zebrafish are viable. We found that at 17 days postfertilization (dpf), we were able to recover wild-type, *rad50*$^{+/-}$, and *rad50*$^{-/-}$ zebrafish in Mendelian ratios (Fig 3.2A). However, at 9 weeks postfertilization (wpf), we failed to recover any *rad50*$^{-/-}$ zebrafish (Fig. 3.2B). The *rad50*$^{-/-}$ zebrafish were still viable at 6 wpf, but they showed a significant size reduction (Fig. 3.2C, 3.2D, and 3.2E). The average length for the 6 wpf *rad50*$^{-/-}$ zebrafish was 1.61 cm, which was significantly smaller than the 2.51 cm length (N=25) for the wild-type and heterozygous siblings (Fig. 3.2D and 3.2E). The 6 wpf *rad50*$^{-/-}$ zebrafish had a mass of 26.83 mg (N=15) on average compared to significantly greater mass of 104.76 mg (N=25) for the wild-type and heterozygous siblings (Fig. 3.2E).

***rad50* mutants are radiosensitive**

Given the role *rad50* plays in DNA repair, we tested to see if our mutants were radiosensitive. 3 wpf *rad50*$^{+/-}$ incross fish were irradiated with 0, 20, or 40 Gy of ionizing X-ray radiation and then monitored for survival over the course of three weeks. The unirradiated group survived for the entire three-week period (data not shown). At 20 Gy, *rad50*$^{-/-}$ zebrafish all perished by 9 days postirradiation (dpi) while roughly 70% of the wild-types and heterozygotes survived the three-week time period (Fig. 3.3A). At 40 Gy, *rad50*$^{-/-}$ zebrafish all perished by 7 dpi while wild-types and heterozygotes perished by 13 dpi (Fig. 3.3B).

Since loss of *rad50* does not decrease γH2AX, a western blot was performed for γH2AX following 15 Gy of irradiation with ionizing X-rays of 7 dpf wild-type, *rad50*$^{+/-}$,

and *rad50*$^{-/-}$ zebrafish. Samples were collected 5 hours, 24 hours, or 48 hours postirradiation (hpi). The *rad50*$^{-/-}$ samples showed γH2AX staining at each time point, while the wild-type and *rad50*$^{+/-}$ samples showed lower staining at each time point compared to the mutants (Fig. 3.3C). It was further determined that in wild-type zebrafish, γH2AX shows strongest staining at 3 hpi and then decreases over time, completely disappearing by 18 hpi (Fig. 3.3D). Repeating the experiment with 5 dpi wild-type and *rad50*$^{-/-}$ zebrafish, again irradiating with 15 Gy but collecting samples at 18 hpi, there was strong staining of γH2AX for the *rad50*$^{-/-}$ sample but none for the wild-type sample (Fig. 3.3E).

rad50 mutants have leukocytopenia starting at 3 wpf

Using whole-mount RNA *in situ* hybridization (WISH) for hematopoietic stem cell (HSC) markers *cmyb* and *runx1*, we found that the *rad50*$^{-/-}$ mutants did not have any defect in the emergence of HSCs (Fig. 3.4A). No defect was observed in migration or colonization of adult HSC niche in the kidney or thymus in the *rad50*$^{-/-}$ mutants using *cmyb* and *rag1* as markers for WISH (Fig.3. 4B). While there were no defects in the emergence of colonization of HSCs, there was a defect in the hematopoietic system of the *rad50*$^{-/-}$ zebrafish at 3 wpf. The fish showed a marked reduction in the number of pan-leukocytes compared to wild-type and heterozygous siblings (Fig. 3.4C). This was determined through whole-mount immunofluorescence with an antibody against zebrafish L-plastin, a pan-leukocyte marker and using confocal microscopy examining the tails of the zebrafish.

Discussion

The *rad50*$^{-/-}$ zebrafish are the first viable vertebrate model for a null *rad50* mutation. *Rad50*, a member of the MRN complex, is conserved in archaea like *Pyrococcus furiosus* and has an ortholog present in prokaryotes called SbcC [219,220]. *Rad50*-mutant mice are embryonic lethal, with the embryos appearing smaller and being reabsorbed starting at E6.0 through E8.5 [74]. In zebrafish, *rad50* is maternally provided; we verified this via quantitative real-time PCR (data not shown). Given that *Rad50*-mutant mice fail early in development, we hypothesize that the only reason the *rad50*$^{-/-}$ zebrafish are viable is due to maternal effect because the maternal supply of *rad50* is present during early embryonic development. We were not able to generate a maternal-zygotic null for *rad50* and did not find any mutant phenotypes prior to 5 dpf.

The maternal effect for *rad50* was a bit of a double-edged sword for us. While it likely is what allowed us to recover viable *rad50* mutants, it made study of the early development effects of *rad50* in zebrafish impossible. Because *rad50* mutants never reached breeding size, and the attempts we made to breed them were all unsuccessful, we could not use *rad50*$^{-/-}$ females to bypass maternal effect. We explored several transgenic approaches to bypass maternal effect. We put *rad50* under the control of two different promoters that do not have maternal effect, heat shock protein 70 and ubiquitin. However, neither of these promoters allowed us to recover normal-sized *rad50* mutants. We also attempted gene targeting to generate a floxed *rad50* allele, but this technology is still in its infancy in zebrafish, and we failed to recover any zebrafish with successfully targeted alleles in *rad50*.

***rad50* mutants are radiosensitive**

Both human and mouse cells that are mutant for *Rad50* are radiosensitive [74,221]. *rad50*-mutant zebrafish are also radiosensitive by irradiating 3 wpf *rad50*$^{+/-}$ incross fish with two doses of radiation: 20 and 40 Gy. We found that the *rad50*$^{-/-}$ fish died significantly earlier than the wild-type and heterozygous siblings. We also found that *rad50*$^{-/-}$ zebrafish showed more γH2AX staining following irradiation and showed staining for longer. γH2AX, phosphorylated histone H2AX, is a marker of DNA damage [222]. Histone H2AX is phosphorylated by ATM [222]. In two different *rad50* mouse mutants, the *Rad50*^{S} allele and a hook domain mutation, *Rad50*^{46}, *ATM* is overactivated [77,217]. Further, mutating *ATM* in these *Rad50*-mutant backgrounds results in a less severe phenotype than in either *Rad50* mutation alone [77,217]. Further, it has been shown that Rad50 is phosphorylated by ATM, an event that regulates both the cell cycle and DNA repair, further illustrating the key interactions between these two proteins [223].

Since histone H2AX is phosphorylated by ATM kinase, there are two alternative hypotheses to explain the increased γH2AX seen in the *rad50* mutants: increased DNA damage or overactivation of *ATM*. There is constitutive γH2AX in the *Rad50* hook domain mouse mutants *Rad50*$^{+/46}$ and *Rad50*$^{+/47}$ [217]. Phosphorylation of γH2AX was also observed in the absence of irradiation in the *Rad50*$^{S/S}$ mice [77].

ATM is constitutively expressed and is not up-regulated in response to DNA damage [224]. Instead, ATM is regulated posttranslationally via autophosphorylation at serine 1981, which is considered a marker for ATM activation [225]. This means that to monitor ATM activation, an antibody against the phosphorylated form is required. This antibody does not exist in zebrafish, consequently we could not easily determine if there

was increased activation of *ATM* in our *rad50*$^{-/-}$ zebrafish.

Unlike in mice, mutating *tp53* does not rescue the *rad50*-mutant zebrafish

In the *Rad50*$^{S/S}$ mice, mutating *tp53* provided a partial rescue to the hematopoietic failure and size defect [76]. However, crossing our *rad50* mutants into a *tp53*$^{zdf1/zdf1}$-mutant background failed to rescue the defects seen in the *rad50*$^{-/-}$ zebrafish (data not shown). We have found that *tp53*$^{zdf1/zdf1}$-mutant background does rescue the sex determination defect we see in our *xrcc2*$^{-/-}$ mutants (manuscript submitted). It is possible that the *tp53*$^{zdf1/zdf1}$-mutant background fails to rescue our *rad50*$^{-/-}$ zebrafish while it does rescue the *Rad50*$^{S/S}$ mice because the zebrafish *rad50* mutation is a null while the *Rad50*^{S} allele is not. It could also stem from the differences in hematopoiesis in mammals compared to fish. The hematopoietic stem cells develop in the bone marrow in mammals (and all terrestrial vertebrates), while they reside in the kidney in zebrafish.

The *rad50* mutants have hematopoietic defects

There were no defects with HSC emergence or colonization of the thymus or kidney, the adult niches in zebrafish. These results are not surprising given the fact that both of these events occur early enough in development that maternal effect is still likely occurring for *rad50*. We did not observe a phenotype for the hematopoietic system until 3 wpf at which point we observed a significant decrease in the number of leukocytes. We did not perform IHC to look for defects in the HSC population at 3 wpf. We hypothesize what is occurring is an accumulation of DNA damage in the rapidly dividing HSCs that leads to apoptosis of the HSCs given that they are missing an important DNA repair

factor in *rad50*. In both the *Rad50*^{S} and *Rad50*^{46} hypomorphic *Rad50* mouse mutants, there are defects in the primitive hematopoietic cells and germ cells [76,77,217]. The stem cells from *Rad50*^{S} mutants cannot reconstitute the bone marrow in lethally irradiated wild-type mice [77]. There is also evidence that *ATM* activation may play a role in anemia. *ATM* activation has been implicated in Diamond-Blackfan Anemia (DBA) in zebrafish [226]. DBA is an anemia caused by impaired RNA processing due to a deficiency in ribosomal proteins and involves the DNA damage repair pathway [226,227]. Since we hypothesize there is overactivation of *ATM* in our *rad50* mutants based on results from two mouse *Rad50* mutants, this may be contributing to the hematopoietic defects that we are seeing.

To determine if the *rad50*-mutant size defect was due to hematopoietic failure, we attempted to rescue the *rad50*$^{-/-}$ fish by performing an HSC transplant experiment. It has been shown that HSC transplant allows lethally irradiated fish to survive hematopoietic failure [228]. However, we were unable to successfully rescue with an HSC transplant. It is not clear if this was due to technical failures due to the complicated nature of the experiment, or if the transplant does not rescue. It did not appear that the transplanted HSCs colonized the kidney in the *rad50* mutants (data not shown). This would suggest a technical failure, and it may be worth repeating this experiment in the future. If we are able to successfully perform an HSC transplant experiment, it will offer insight into the mechanism for the small size of the *rad50* mutants. The fish would be *rad50*$^{-/-}$ in every cell type except for in the hematopoietic system, so if they reach a normal size, it would suggest that the hematopoietic defects were the cause of the small size. However, if they are still smaller than normal, it would suggest some cell intrinsic defect, such as increased

apoptosis or decreased cellular proliferation.

First viable model of a null mutation in *rad50* in a vertebrate

We were able to generate the first viable vertebrate model of homozygous *rad50* null mutation. In our model, we were able to recapitulate some clinical features seen in NBS, namely decreased size, radiosensistivity, and hematopoietic failure. Given the similarities between *ATM*, *MRE11*, *NBN*, and *RAD50* mutant phenotypes, zebrafish may prove to be a great model system to study mutations in those other genes as well.

While we were able to learn some roles for *rad50* in zebrafish from our mutants, technical challenges associated with these mutants stemming from maternal effect, difficult experiment techniques, and lack of key reagents have left many open questions about the mechanism for the effects of the *rad50*-mutant phenotype we observed.

Materials and methods

Ethics statement

All animals used in this study were used in accordance with the policies of the University of Utah Institutional Animal Care and Use Committee following approved protocol 16-03003.

Animals

Transcription activator-like effector nuclease (TALEN) mutagenesis was performed to generate the *rad50* zebrafish mutants [114]. The *rad50* TALENs were generated by the Utah Mutation Generation and Detection core facility with the following

recognition sequences: *rad50* TALEN L: ACATCACATCAGGAGACT *rad50* TALEN R: GGACAAAAGTGTTTCCTTT. Zebrafish were housed at the CZAR (Centralized Zebrafish Animal Resource) facility at the University of Utah.

Genotyping of *rad50* mutants

rad50 mutants were genotyped using polymerase chain reaction (PCR) and high-resolution melting curve analysis (HRMA) [179–181]. Isolation of genomic DNA was carried out by alkaline lysis (incubation in 20-40 µl of 50 mM NaOH at 95 °C for 20 minutes, followed by addition of 2-4 µl of 1M Tris pH 8.0). PCR primers were as follows: *rad50* F TTTTTGCAGACCATCATTGAG and *rad50* R TCAATGACTTACTTTGGGATCA. LCGreen Plus+ Melting Dye [BioFire Defense BCHM-ASY-0005] was added to the PCR reaction to perform HRMA. PCR conditions were: 2’ 95 °C; 45 cycles of 10” 95 °C, 15” 62 °C, 10” 72 °C; followed by 2’ 95 °C then hold at 12 °C. The PCR product size is 105 bp for wild-type and 98 bp for the 7-bp deletion mutant. HRMA was used to analyze the completed PCR reaction with a temperature range of 70 °C to 95 °C on a LightScanner HR I 96 [Idaho Technology Inc.] using small amplicon-based genotyping for melting curve data analysis.

Radiation survival

rad50$^{+/-}$ were incrossed and 3 wpf fish were irradiated with 0, 20, or 40 Gy using ionizing X-ray radiation. The fish were separated based on radiation dose and not by genotype. The irradiated and unirradiated fish monitored for survival over the course of three weeks checking in the morning when the lights came on at 9 a.m. and before the

lights went out at 11 p.m. Dead fish were made into DNA and genotyped following the protocol previously described above.

Western blot analysis

To detect γH2AX, a western blot was performed for γH2AX was performed with GAPDH used as the loading control. 7 dpf wild-type, *rad50*$^{+/-}$, and *rad50*$^{-/-}$ zebrafish were irradiated with 15 Gy of ionizing X-rays. Irradiated zebrafish embryos were collected 5 hours, 24 hours, and 48 hours postirradiation (hpi). Each embryo needed to be genotyped, so the tail was made into DNA and genotyped following the above protocol. The rest of the embryo was placed into complete radioimmunoprecipitation assay (RIPA) buffer (1% Nonide P-40, 0.5% sodium deoxycholate, 0.1% sodium dodecyl sulfate) containing 1% protease inhibitors (Sigma P8340) and 1% benzonase (Novagen 70746-3) and were homogenized using a Kontes Pellet Pestle Motor. Protein concentrations were determined by the BCA assay kit (Thermo Scientific 23227). The western blot used precast denaturing gels (Novex NP0301BOX) and 25 μg of protein was loaded. A prehydrated PVDF membrane (GE PV4HYA0010) was used for the transfer. The membrane was blocked with 3% bovine serum albumin (Amresco 0332) in 1X tris-buffered saline with 1% tween-20 (TBST). The blot was stained with anti-Phospho-Histone H2A.X (Ser139) at 1:2,000 and anti-GAPDH antibody (Abcam 9484) at 1:2,000 in block and incubated overnight at 4 °C. Washes were carried out in 1x TBST four times for five minutes each. For anti-Phospho-Histone H2A.X (Ser139), anti-rabbit-horseradish peroxidase secondary (Cell Signaling 7074S) was used, and for anti-GAPDH, anti-mouse-horseradish peroxidase secondary antibody (Cell Signaling 7076S). Each

secondary antibody was used at 1:5000 in the same block used for the primary antibodies. The secondary antibodies were incubated at room temperature for 30 minutes. The blot was washed five times for 10 minutes each in 1x TBST. Following washing, the blot was treated with chemiluminescent horseradish peroxidase substrate (Millipore WBKLS0500) and exposed to film (ThermoFisher Scientific 34090) to detect protein signal.

Whole-mount RNA *in situ* hybridization (WISH)

Previously described protocols were followed for WISH [229,230].

Whole-mount immunofluorescence

Using *rad50*$^{+/-}$ embryos at 2 and 3 weeks postfertilization, whole-mount immunofluorescence was performed following previously described protocols using an anti-L-plastin antibody at 1:10,000 dilution followed by the secondary antibody Alexa Fluor 488 Goat Anti-Rabbit IgG (Abcam 150077) at a 1:1,000 dilution [231,232].

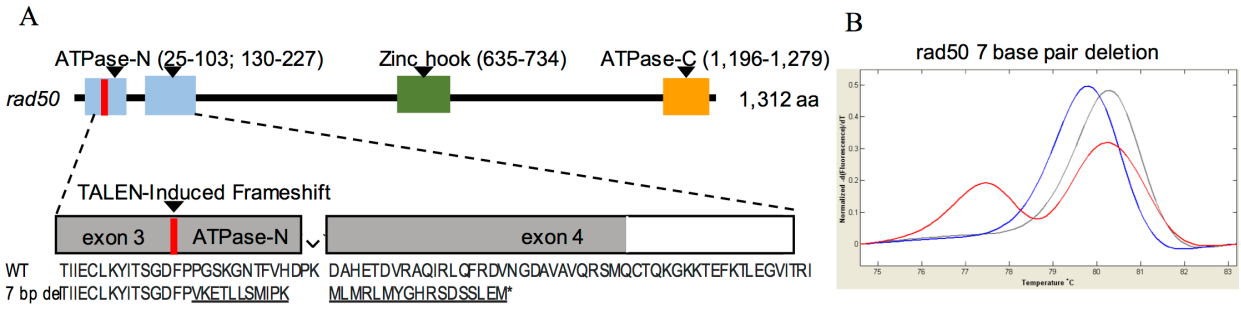

Figure 3.1. TALEN-induced frameshift mutation in zebrafish *rad50*. (A) Zebrafish *rad50* gene structure showing the TALEN cut site in the third exon disrupting the ATPase-N domain. Genotyping primers for *rad50* labeled F and R indicate the forward and reverse primers. A 7-base-pair (bp) deletion in *rad50* was generated through TALEN mutagenesis with the resulting amino acid changes that occur in exons 3 and 4 including the premature stop codon. (B) HRM genotyping curves of a wild-type, heterozygote, and homozygote for the *rad50* 7-bp deletion allele using the primers shown in (A).

Figure 3.2. *rad50* mutants are juvenile lethal with a growth defect. Genotyping was performed via HRM with grey representing wild types, red for *rad50*$^{+/-}$, and blue for *rad50*$^{-/-}$. (A) Mendelian ratios were recovered wild type, *rad50*$^{+/-}$, and *rad50*$^{-/-}$ zebrafish from a *rad50*$^{+/-}$ incross at 17 days postfertilization (dpf). (B) No *rad50*$^{-/-}$ zebrafish survived to 9 weeks postfertilization (wpf) out of 20 *rad50*$^{+/-}$ incross progeny. (C) At 6 wpf, a normal Mendelian ratio was recovered with 7 *rad50*$^{-/-}$ zebrafish out of 27 *rad50*$^{+/-}$ incross progeny. 6 wpf *rad50*$^{-/-}$ zebrafish are significantly smaller than wild-type and *rad50*$^{+/-}$ siblings for both length and mass representative images in (D) and quantification in (E). Errors bars represent one standard deviation. Wild-type/*rad50*$^{+/-}$ N=25 *rad50*$^{-/-}$ N=15.

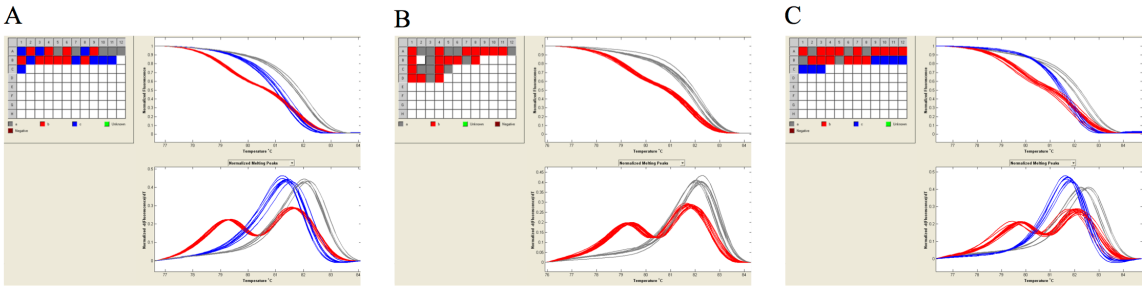
A
B
C

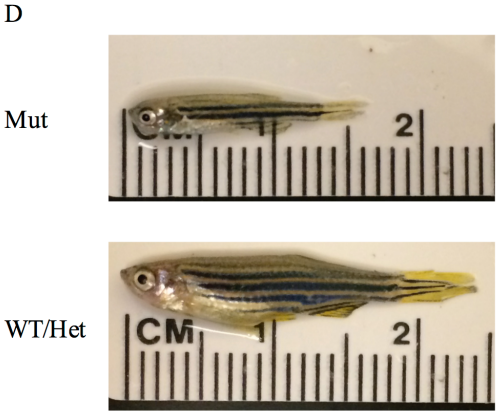
D
Mut
WT/Het
CM
1
2

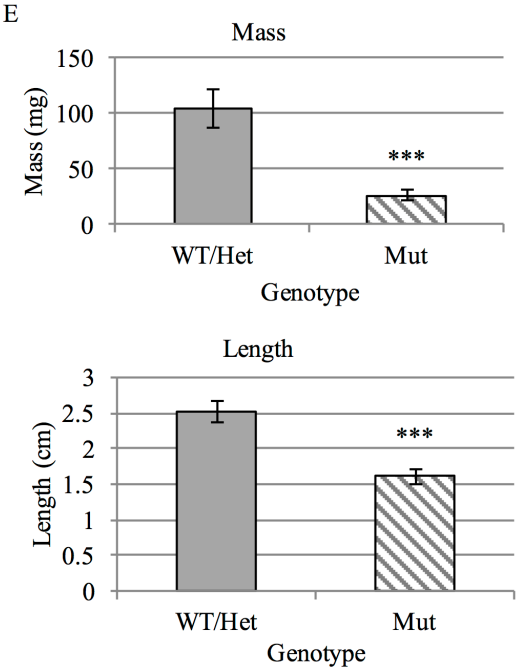
E
Mass
150
100
50
0
Mass (mg)
***
WT/Het
Mut
Genotype
Length
3
2.5
2
1.5
1
0.5
0
Length (cm)
***
WT/Het
Mut
Genotype

Figure 3.3. *rad50*-/- zebrafish are radiosensitive. *rad50*$^{-/-}$ zebrafish die significantly faster than wild-type or *rad50*$^{+/-}$ siblings when exposed to 20 Gy (A) or 40 Gy (B) of ionizing X-ray irradiation. (C) 7 dpf wild-type, *rad50*$^{+/-}$, and *rad50*$^{-/-}$ zebrafish were irradiated with 15 Gy of ionizing X-rays, and a western blot was performed for γH2AX with samples collected 5, 24, and 48 hours postirradiation (hpi). GAPDH was used as the loading control. *rad50*$^{-/-}$ zebrafish showed elevated levels of γH2AX at each time point compared to wild-type and *rad50*$^{+/-}$ siblings. (D) 6 dpf wild-type zebrafish were irradiated with 15 Gy of ionizing X-rays, and a western blot was performed for γH2AX with samples collected 3, 6, 12, 18, and 24 hpi with an unirradiated control. GAPDH was used as the loading control. The wild-type zebrafish cleared γH2AX by 18 hpi. (E) At 18 hpi, 5 dpf *rad50*$^{-/-}$ zebrafish have elevated γH2AX compared to wild-type siblings following irradiation with 15 Gy of ionizing X-rays.

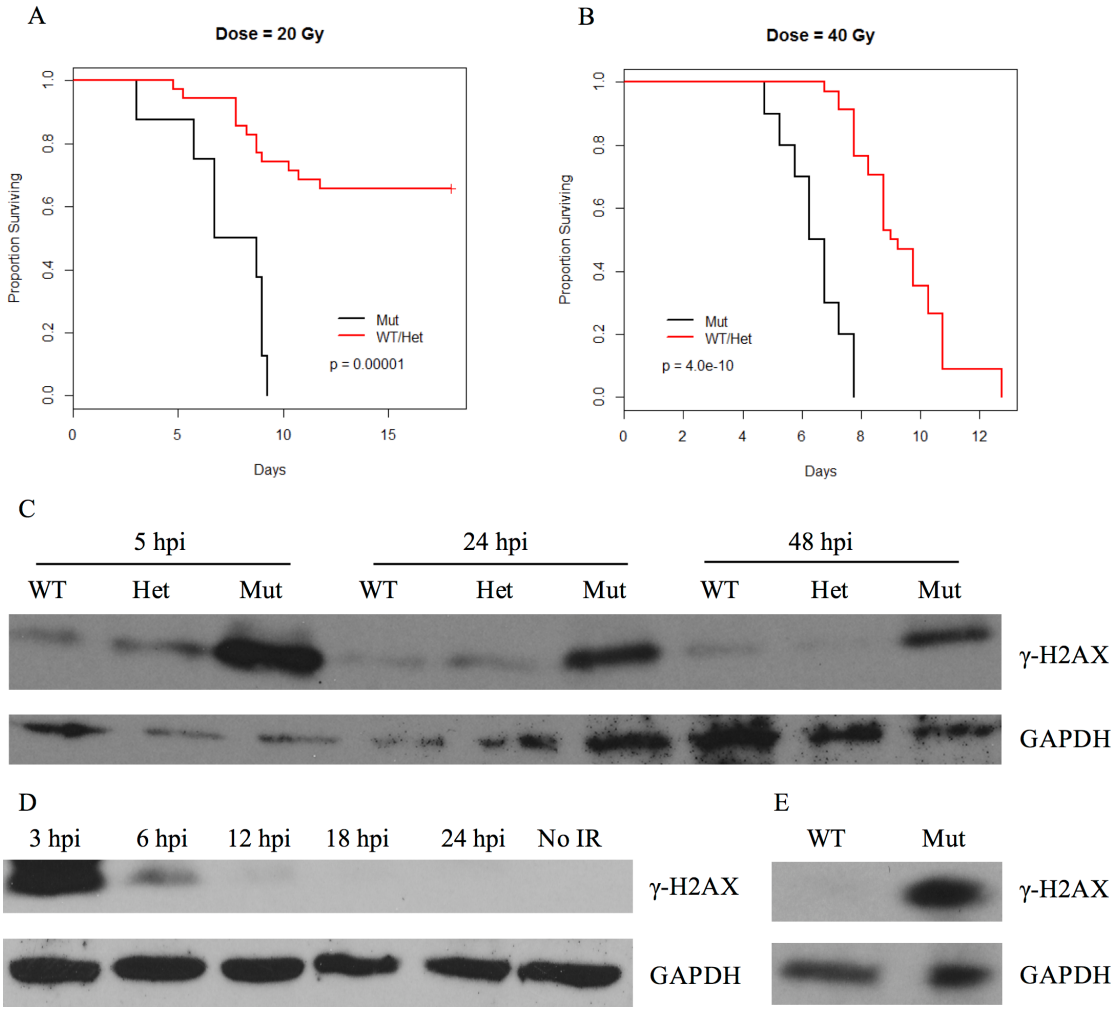
A
Dose = 20 Gy
Proportion Surviving
Days
Mut
WT/Het
p = 0.00001
B
Dose = 40 Gy
Proportion Surviving
Days
Mut
WT/Het
p = 4.0e-10
C
5 hpi
24 hpi
48 hpi
WT
Het
Mut
γ-H2AX
GAPDH
D
3 hpi
6 hpi
12 hpi
18 hpi
24 hpi
No IR
γ-H2AX
GAPDH
E
WT
Mut
γ-H2AX
GAPDH

Figure 3.4. Leukocytopenia occurs in *rad50*-/- beginning at 3 wpf. (A) Whole-mount RNA *in situ* hybridization (WISH) was performed using the hematopoietic stem cell (HSC) markers *cmyb* and *runx1* on 28 to 32 hour postfertilization *rad50*$^{+/-}$ incross embryos. Blue arrows point to HSCs. There was no defect in the emergence of HSCs in *rad50*$^{-/-}$ embryos. (B) 5 dpf *rad50*$^{+/-}$ incross embryos were analyzed for proper HSC migration to the adult niches in the kidney and thymus using WISH for *cmyb* and *rag1*. Blue arrows point to the thymus, and green arrows point to the kidney. 39/41 embryos had proper migration to the kidney and thymus using *cymb*, and 43/43 embryos had proper migration to the thymus using *rag1*. (C) Whole-mount immunofluorescence using an antibody against zebrafish L-plastin, a pan-leukocyte marker, was performed with a confocal microscope examining the tails of 3 wpf *rad50*$^{+/-}$ incross zebrafish. *rad50*$^{-/-}$ zebrafish showed a reduction in the number of leukocytes compared to wild-type and *rad50*$^{+/-}$ siblings.

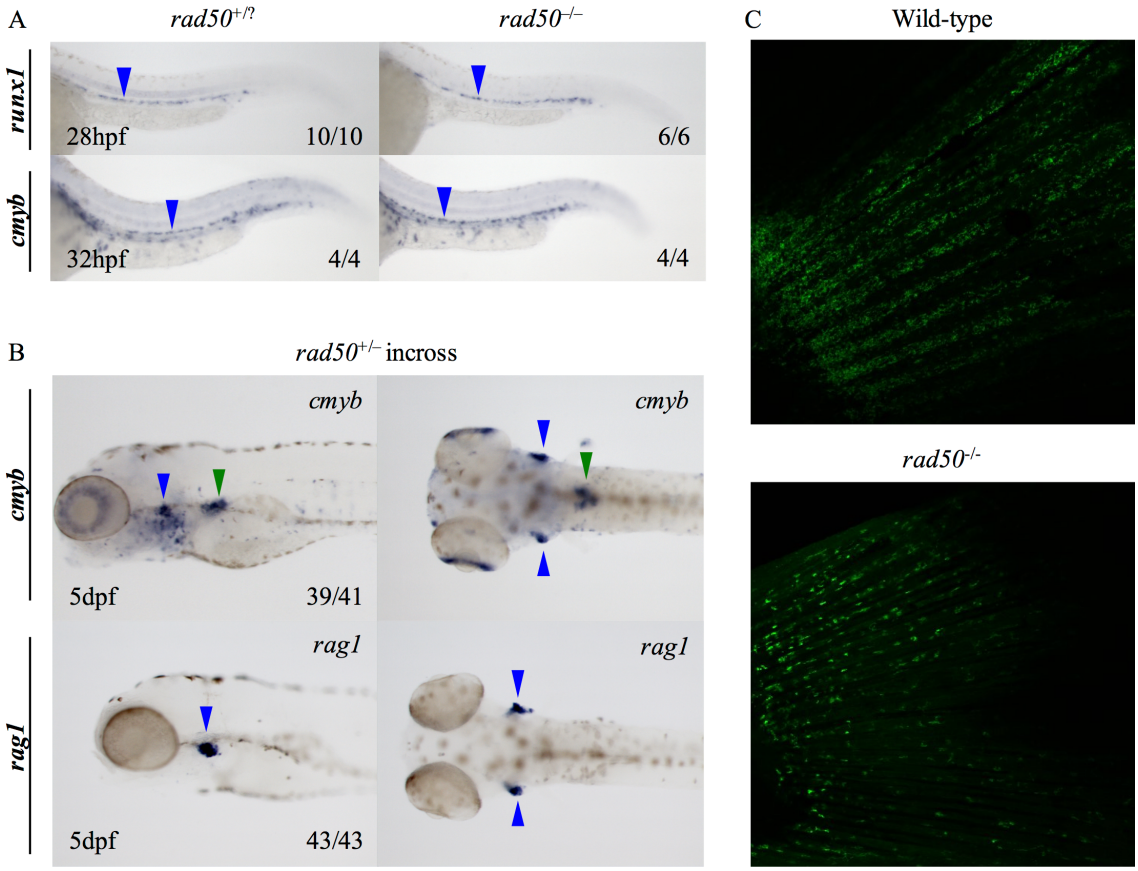
A
rad50+/?
rad50−/−
runx1
28hpf
10/10
6/6
cmyb
32hpf
4/4
4/4
B
rad50+/− incross
cmyb
cmyb
cmyb
5dpf
39/41
rag1
rag1
rag1
5dpf
43/43
C
Wild-type
rad50-/-

CHAPTER 4

CONCLUSION

Zebrafish (*Danio rerio*) have traditionally been used for developmental studies because transparent embryos and external fertilization allow easier study of early steps in development compared to mammalian systems [233]. Zebrafish have also been used for many forward genetic screens [234–237]. With the development of transcription activator-like effector nucleases (TALENs) and CRISPR/Cas9, it is now possible to make targeted mutations and perform reverse genetics in zebrafish, allowing the study of specific genes [114,238–240]. With the advances in reverse genetics techniques available in fish, zebrafish were selected as the model organism to study several strong candidate moderate risk breast cancer susceptibility genes: *RAD50* and *XRCC2*.

RAD50 and *XRCC2* play important roles in DNA double-strand break (DSB) repair [3–5]. Rad50 functions early in the pathway in a complex with Mre11 and Nibrin [7,8]. XRCC2 is a Rad51 paralog that acts specifically in the homology-directed DSB repair (HDR) pathway [38]. In addition to playing a role in DNA DSB repair and breast cancer susceptibility, biallelic mutations in *RAD50* result in Nijmegen breakage syndrome-like disorder, a disorder similar to Nijmegen breakage syndrome (NBS), while biallelic mutations in *XRCC2* result in Fanconi anemia (FA) [50–52]. While they are different diseases, NBS and FA share many clinical features, including acute myeloid leukemia

(AML), bone marrow failure, thumb defects, microcephaly, and growth retardation [53–55,57–67,143,241]. Additionally, there are no viable mouse models that possess bialleic null mutations in either *RAD50* or *XRCC2* [74,148].

Most of what is known about biallelic null mutations in *XRCC2* comes from the Chinese hamster ovary cell line irs1 [43,49,118,242]. A patient homozygous for p.Arg215* nonsense mutation in *XRCC2* had FA [51,52]. There have been multiple studies on Rad50 in mice using missense substitutions that are not null alleles [77,217]. The patient who had NBSLD carried two different *RAD50* alleles, a nonsense mutation (c.3277C→T; p.R1093X) and a lost stop codon mutation (c.3939A→T) that added 66 amino acids to the C-terminus [50]. This patient presented with a Rad50 protein level that is 95% less than a wild-type person [50].

Zebrafish models of *rad50* and *xrcc2* mutations

Since there are no viable mouse models for biallelic null alleles for either gene, zebrafish were chosen as the model system to study the effects that mutations in *rad50* and *xrcc2* play in later vertebrate development. In zebrafish, other HDR pathway genes such as *BRCA2* for which homozygous null mutations result in embryonic lethality in mice, are viable [104,105,243].

rad50 mutants show growth retardation, hematopoietic defects, and radiosensitivity

The *rad50* mutants showed growth retardation beginning at 3 weeks postfertilization (wpf) and were significantly smaller at 6 wpf than wild-type and

heterozygous siblings. Also at 3 wpf, the *rad50*$^{-/-}$ zebrafish showed leukocytopenia. This was determined using an antibody against the pan-leukocytes marker L-plastin and performing fluorescent microscopy to examine leukocytes in the tails of 3 wpf wild-type or *rad50*$^{-/-}$ zebrafish. We hypothesized that hematopoietic stem cell (HSC) failure was the cause of the leukocytopenia since HSC failure has been observed in human NBS and NBS-like disorder patients and mouse *Rad50*$^{S/S}$ mutants [50,53,76]. There were no defects in the emergence of the HSCs or colonization of the adult niches in the kidney or thymus. While the leukocytopenia was never rescued, the growth retardation was likely due to the hematopoietic system defects.

To attempt to rescue the leukocytopenia and possibly size defect, a HSC transplant experiment was attempted. The transplant experiment failed to rescue the *rad50*$^{-/-}$ growth defect or leukocytopenia. Since these experiments are technically challenging, it bears repeating to determine if the first experiment was a technical failure or if an HSC transplant is not sufficient to rescue the *rad50*$^{-/-}$ growth retardation. Another possible experiment would be to express *rad50* under the control of the CD41 promoter, which is expressed in HSCs [244].

rad50 is an important DNA repair factor, and the *rad50*$^{-/-}$ zebrafish showed DNA repair defects. When irradiated with 15 Gy of ionizing radiation, the *rad50*$^{-/-}$ zebrafish failed to clear γH2AX, a marker of DNA damage, compared to wild-type and *rad50*$^{+/-}$ zebrafish. When 3 wpf *rad50*$^{-/-}$ incross fish were irradiated with 20 or 40 Gy, the *rad50*$^{-/-}$ fish died significantly earlier than wild-type and heterozygous siblings.

One possible alternative explanation for the elevated γH2AX is that ATM has been shown to be over-activated in two different mouse *Rad50*-mutant lines [77,217]. ATM

is the kinase responsible for phosphorylating histone H2AX in response to DNA damage, making it γH2AX [222]. It is possible that γH2AX was hyperphosphorylated due to overactivation of ATM, as was observed in mice [77,217]. From the radiation survival experiments, we showed that *rad50*-mutant zebrafish are radiosensitive. The increased γH2AX seen in *rad50* mutants is likely due to either a failure to clear γH2AX due to a DNA repair defect, overactivation of ATM, or a combination of both.

As ATM is regulated posttranslationally through phosphorylation at serine 1981, monitoring for ATM over-activation requires a method to differentiate between phosphorylated and unphosphorylated ATM [225]. An antibody for phospho-serine 1981 in ATM does not exist in zebrafish, but it may be possible to perform mass spectrometry instead to determine if ATM is over-activated in the *rad50*$^{-/-}$ zebrafish [245]. A kinase-inactive zebrafish ATM has shown to act as a dominant-negative for ATM function in both human and zebrafish cells [246]. Constitutively expressing this allele in the *rad50*$^{-/-}$ mutants might mitigate some of the mutant phenotypes as has been observed in mice [77,217]. Because the *rad50*$^{-/-}$ zebrafish are the only vertebrate model of biallelic null *rad50* mutations, many more questions can be answered using these zebrafish than with missense substitutions due to the possibility of gain-of-function phenotypes, which has been posited for the *Rad50*^{S} allele [77].

Female-to-male sex reversal and seminomas observed in *xrcc2* mutants

xrcc2$^{-/-}$ zebrafish showed female-to-male sex reversal. *xrcc2*$^{-/-}$ females were rescued using a *tp53 zdf1* allele mutant background. Both of these findings are consistent with results obtained with other FA genes, namely *brca2*, *fancl*, and *rad51* in zebrafish

studies [104,121,125].

Expression of *xrcc2* was significantly higher in the gonads of adult male and female wild-type zebrafish than in flank, gut, and head. In *xrcc2*$^{-/-}$ male zebrafish, expression changes in the gonad showed decreased *anti-Müllerian hormone* (*amh*) and *doublesex and mab-3 related transcription factor* 1a (*dmrt1a*) and increased insulin-like growth factor 3 (*igf3*). These expression changes are consistent with increased follicle-stimulating hormone (Fsh) levels, which promotes spermatogenesis in zebrafish [163]. However, there were no consistently observed histologic differences between wild-type and *xrcc2*$^{-/-}$ testes.

30% of *xrcc2*$^{-/-}$ male zebrafish developed seminomas, a testicular germ cell tumor (TGCT), by 22.5 months of age. A seminoma was also observed in a *brca2*$^{-/-}$ zebrafish [104]. In humans, 95% of seminoma patients survive for at least 10 years [170]. However, a subset of about 3% of seminoma patients have treatment-refractory tumors that do not respond to the standard treatment of platinum-based chemotherapy agents (e.g., cisplatin) and have a poor prognosis [170–173]. Whole-exome sequencing was performed on 43 TGCT tumors; of these 43 TGCTs, 2 were treatment-refractory tumors [172]. Both of these treatment-refractory TGCTs contained an *XRCC2* mutation, while none of the nonresistant tumors contained an *XRCC2* mutation [172]. To date, this is the only *xrcc2*$^{-/-}$ model to develop seminomas.

Because of the whole-exome sequencing results showing that XRCC2 may play a role in treatment resistance in TGCTs, the *xrcc2*$^{-/-}$ seminomas need to be evaluated for cisplatin resistance. The sample size from Litchfield et al. [172] was limited to only 2 treatment-refractory TGCTs and was not mechanistic in nature. We have a model that

allows us to test what role if any *xrcc2* plays in cisplatin resistance in TGCTs, which could enable exploration of the resistance mechanism in addition to increasing the sample size. Further, if the tumors are cisplatin-resistant, drug screens could then be performed to determine which drugs might be effective for treatment-refractory TGCTs instead.

The two most commonly mutated genes in TGCTs are *KIT* and *KRAS* [172]. Since it takes almost two years for the seminomas to develop in the *xrcc2*$^{-/-}$ males, it may be possible to decrease the time for tumorigenesis to occur using activated *KRAS* under the control of a gonad-specific promoter (e.g., *vasa* or *ziwi*) [247–249]. Such a model would be more beneficial for research if we could decrease the tumor latency and increase the percentage of fish that develop tumors. Mutating an additional gene known to be mutated in human TGCTs might also create a more faithful model of human *XRCC2*-mutant seminomas.

Zebrafish *rad50* and *xrcc2* mutants show different phenotypes despite similarities in humans

Despite the high degree of similarity between FA and NBS in humans, the zebrafish models of FA and NBS-like disease showed marked differences. Growth retardation and bone marrow failure are clinical features of both diseases, yet only the *rad50* mutants showed these phenotypes [53–57,61–63]. *xrcc2*-mutant zebrafish showed expression changes consistent with elevated Fsh, a feature of both diseases [69,70]. The growth retardation present in the *rad50* mutants made gonad dissection impractical, so it was not tested if there were similar expression changes present in the *rad50* mutants. While both *rad50* and *xrcc2* are involved in DNA repair, only *rad50*$^{-/-}$ zebrafish showed

DNA repair defects. This could stem from the fact that *rad50* is involved early in DNA DSB repair compared to *xrcc2*, which is only involved in HDR [3–5]. Since *rad50* is involved in both NHEJ and HDR, it could explain why the *xrcc2* mutants have a much less severe phenotype compared to the *rad50* mutants, which have many more organ systems affected [115].

Issues with missense substitution assay development

Zebrafish offer several experimental benefits over mammalian organisms to study missense substitutions. mRNAs containing either wild-type sequence or various missense substitutions can be injected into one cell stage embryos. Embryo injection assays in zebrafish have been used for sequence variant functional analysis previously [108,109,250–252]. Davis et al. [253] reviewed the potential that zebrafish possess for analysis of human mutations. Drost and de Wind [110] developed a PCR-based method for generation of mRNAs that does not require cloning or sequencing of the variants, which could accelerate and reduce the costs for evaluation of many sequence variants in parallel. Zebrafish microinjection of mRNAs can therefore be a medium throughput assay, which is preferable to painstaking process of generating mice bearing various missense substitutions.

Because of some biological differences between mammals and zebrafish, it was not possible to assay human missense substitutions using the zebrafish models. The main difficulty was that maternal effect was present for both *rad50* and *xrcc2*, which precluded early embryo assays without a strategy to circumvent the maternal mRNA.

Maternal effect masks early effects of the mutations

The main issue with using zebrafish to study early development is maternal effect, wherein mRNA and protein for some genes are maternally provided in the oocyte, meaning that zebrafish embryos that are genetically null are phenotypically wild type due to the maternal supply of wild-type mRNA [254]. All of the DSB repair genes appear to have maternal effect; the presence of maternal mRNA for both *rad50* and *xrcc2* was confirmed via quantitative reverse transcription polymerase chain reaction (data not shown). To perform the mRNA injection assays, maternal mRNA cannot be present. The wild-type maternal RNA/protein masks any decrease in function that the variants might cause in the assays due to the wild-type maternal protein complementing the mutant phenotypes.

Using homozygous mutant mothers is the easiest way to bypass maternal effect. However, it was not possible to generate fertile *rad50* mutants since the mutants suffered from growth retardation. Further, there is evidence from mice that *Rad50* hypomorphic mutants have severe fertility defects [77,217]. For *xrcc2*, mutant females were eventually recovered, but other issues prevented assay development from occurring; these will be discussed later.

Mutating *tp53* has been shown to partially rescue *Rad50* and FA mutants [76,104,121]. However, only the *xrcc2*-mutant phenotype, and not the *rad50*-mutant phenotype, could be partially rescued through *tp53* mutation. $xrcc2^{-/-}$ females were rescued by utilizing the dominant-negative *zdf1* mutant allele of *tp53*. Despite evidence that *tp53* partially rescues $Rad50^{S/S}$ mice, no differences were observed between $rad50^{-/-}$ zebrafish and $rad50^{-/-}$; $tp53^{zdf1/zdf1}$ zebrafish.

Since mutating *tp53* did not rescue the *rad50*$^{-/-}$ zebrafish, several different approaches, using transgenes and gene targeting, were attempted to try to bypass maternal effect. An approaching using the ubiquitin promoter targeted to a phiC31 site that has been verified to express ubiquitin-driven transgenes was attempted to drive human *RAD50* in zebrafish [255,256]. The goal was to recover a chimera that did not express *RAD50* in the germline but was normal sized. However, the fish that were *rad50* mutants and had incorporated the transgene were all growth retarded (data not shown). The approach we felt had the best chance to work was to make a *rad50* floxed allele and use an oocyte-specific promoter, e.g. *ziwi*, to drive Cre [247]. This approach would bypass maternal effect without affecting other organs in the female zebrafish. It also would remove *rad50* after crossing over, decreasing the chance to negatively affect fertility [247]. However, when this work was attempted, little had been done on gene targeting in zebrafish, so we were never able to recover a *rad50* allele that included LoxP sites. Because each of the transgenic approaches to bypass maternal effect failed, we were unable to bypass maternal effect for *rad50*, meaning we were unable to conduct our assays of missense substitutions in human *RAD50*.

Because of maternal effect, we were unable to observe any mutant phenotypes prior to 5 dpf. Multiple experiments were attempted earlier in development, but no different in phenotype was observed in the *rad50*$^{-/-}$ zebrafish compared to wild-type siblings. These assays included whole-mount immunofluorescence for cleaved Caspase-3, a marker of apoptosis, following irradiation with doses ranging from 10-100 Gy of ionizing X-rays [111]. Cleaved Caspase-3 staining showed no difference between *rad50* mutants compared to wild-type siblings for experiments performed on 1-3 dpf embryos.

The amount of cleaved Caspase-3 decreased considerably each day and was nearly undetectable by 4 dpf even with 100 Gy of radiation due to development of the notochord [257]. Another assay that was attempted was using 5-bromo-2'-deoxyuridine (BrdU) to monitor differences in cell proliferation at 3 dpf. However, there was no difference in BrdU in *rad50* mutants compared to wild-types. The last assay that was attempted radiation-induced cell cycle arrest. This assay was not feasible in later embryos because approximately 90% of the cells were in G_0/G_1 at 3 dpf, so we did not observe differences in cell cycle arrest between *rad50*$^{-/-}$ and wild-types or between wild-types that received different doses of radiation (from 15-75 Gy of ionizing X-rays) (data not shown).

xrcc2 loss appears to only affect the gonad

While mutation of *tp53* eventually allowed for the recovery of *tp53*$^{zdf1/zdf1}$; *xrcc2*$^{-/-}$ females, thus bypassing maternal effect for *xrcc2*, assays for human *XRCC2* sequence variants were still not possible. Zebrafish rely more heavily on NHEJ compared to HDR to repair DSBs [258,259]. This is likely related to the fact that zebrafish lack *brca1* and have an incomplete *bard1* that lacks the N-terminal RING domain required for heterodimerization with *brca1* (SVT unpublished) [28,260]. There is a hypothesis in the field that *BRCA1* inhibits NHEJ, which is supported by evidence in mice that mutation of 53BP1, an important NHEJ factor that also blocks strand resection, an important process in HDR, partially rescues Brca1-mutant cells [261].

The expression of *xrcc2* appears to be limited to the gonad in adult zebrafish. Prior to our study of *xrcc2*, there have been no previous studies of *xrcc2* in zebrafish. More research will be necessary to elucidate the expression of *xrcc2* throughout

development in zebrafish. The limited expression of *xrcc2* could stem from the fact that zebrafish lack *brca1*, leading to a globally reduced dependence on HDR relative to NHEJ [260,262,263].

A previous study reported repair of damaged GFP at relatively high frequency, and the amount of functional *EGFP* produced was significantly decreased following injection of a *rad51* morpholino [113]. However, we were not able to replicate these findings. Using plasmids provided by the Jun Chen lab, we were unable to generate *EGFP* repair at levels even remotely close to what Liu et al. [113] reported. Additionally, *xrcc2* maternal-zygotic mutants showed only a 13% reduction in *EGFP* compared to wild-types (data not shown). This finding sits in stark contrast to the roughly 3-fold decrease that was observed with the injection of the *rad51* morpholino [113]. Since *xrcc2* is a rad51 paralog, it would seem logical that a similar decrease in *EGFP* production would be observed in the *xrcc2* mutants compared to the *rad51* morpholino-injected fish. However, there are a few possible explanations for the differences observed between our study and Liu et al. [113]. First, the zebrafish field has moved away from morpholinos because of the off-target effects associated with morpholinos that can yield inaccurate results [264–267]. Now that *rad51* mutants exist for zebrafish, this finding could attempt to be replicated in the mutant background [125]. Further, the *rad51*-mutant zebrafish show a more severe mutant phenotype that affects many more organ systems than observed in the *xrcc2*-mutant zebrafish, which could relate to the limited expression of *xrcc2* in zebrafish. In humans, *RAD51* is the only dominant FA gene [79,80]. Lastly, the difference in findings could stem from that fact that we were unable to replicate any of their findings, including the amount of *EGFP* produced in wild-type zebrafish.

Another potential assay explored for the *xrcc2* mutants was sensitivity to DNA damaging agents, including DNA crosslinking agents and ionizing X-rays, which cause DSBs. The irs1 cell line, where *XRCC2* was first discovered, is sensitive to both types of DNA damaging agents [43]. Differences in apoptosis were examined following treatment with DNA damaging agents, using whole-mount immunofluorescence for cleaved Caspase-3 [111]. The DNA damaging agents used were ionizing radiation and cisplatin, a DNA crosslinking chemotherapy drug. Despite the sensitivity of the irs1 cells to these agents, no differences in cleaved Caspase-3 were found in the *xrcc2* mutants compared to wild-types (data not shown).

Given the lack of discernible phenotypes outside of the gonads in the *xrcc2*-mutant zebrafish and the limited expression of *xrcc2* in wild-type adult zebrafish, the possibility exists that *xrcc2* is dispensable outside the gonad. Further, the *xrcc2* mutants show a less severe phenotype when compared to *brca2* mutants, which is also involved in HDR [104]. The tumor spectrum in the *brca2* mutants includes seminomas, a germ cell tumor, papillary cystadenomas, and undifferentiated stromal cell tumors, both somatic cell tumors. Comparatively, *xrcc2* mutants only develop seminomas. Since the mutant phenotypes in *xrcc2*, including both the sex reversal phenotype and tumorigenesis, are largely restricted to the germ cells, we hypothesize that *xrcc2* may function only in crossing over in zebrafish. All of this occurs in cells that lack BRCA1, which plays a central role in DNA repair in most vertebrates, nematodes, and plants [268–270]. Given the fact that *brca1* is a Fanconi anemia gene, it is logical to hypothesize that other compensatory changes might have occurred in concert with the loss of *brca1* in zebrafish to prevent the sex reversal phenotype observed in every other FA gene mutated in

zebrafish [78,104,121,125]. These other potential changes would suggest that the DSB repair pathway may function in subtly different ways in zebrafish compared to mammals, despite the pathway being largely conserved outside of *brca1*, which could explain why the loss of *xrcc2* only appears to affect crossing over [102,260].

Future directions

Because zebrafish rely so much more heavily on NHEJ to repair DSBs, zebrafish were likely not an appropriate model to assay missense substitutions in HDR genes. The *xrcc2*-mutant zebrafish certainly provided some utility to study the effects *xrcc2* plays on vertebrate gonad development. Human cells or the Chinese hamster ovary cell line irs1 likely would have been a better system to assay *XRCC2* mutations; however assays for *XRCC2* mutations have already been performed in irs1 cells [118].

Since zebrafish lack *brca1*, it could be possible to inject human BRCA1 mRNA along with BARD1 mRNA or make transgenic zebrafish that express full-length human BRCA1 and BARD1 cDNA. Based on other literature, this might increase HDR in the zebrafish and might make the damaged GFP assay more meaningful [261,271]. The possibility also exists that *xrcc2* loss could be more severe in zebrafish with human BRCA1 and BARD1 present due to an increased reliance on HDR.

Our lab has had success using human cell lines to assay missense substitutions in the RING and BRCT domains of BRCA1 (manuscript in revision; bioRxiv 092619). For the RING domain, a mammalian 2-hybrid assay was performed with BRCA1 RING fused to GAL4 and BARD1 RING fused to VP16. The interaction between the RING domains is important for BRCA1 function and stability [272,273]. Since both RAD50 and

XRCC2 protein exist in complexes, it may be possible to adapt the mammalian 2-hybrid approach developed for the BRCA1 RING domain for RAD50, examining interactions with Mre11 and Nibrin, and XRCC2, for the interactions with RAD51B, RAD51C, and RAD51D [41,184].

REFERENCES

1. Paul, A. & Paul, S. The breast cancer susceptibility genes (BRCA) in breast and ovarian cancers. *Front Biosci (Landmark Ed)* **19,** 605–18 (2014).

2. Pollard, J. M. & Gatti, R. A. Clinical radiation sensitivity with DNA repair disorders: an overview. *Int. J. Radiat. Oncol. Biol. Phys.* **74,** 1323–31 (2009).

3. Lieber, M. R. The mechanism of double-strand DNA break repair by the nonhomologous DNA end-joining pathway. *Annu. Rev. Biochem.* **79,** 181–211 (2010).

4. Chapman, J. R., Taylor, M. R. G. & Boulton, S. J. Playing the end game: DNA double-strand break repair pathway choice. *Mol. Cell* **47,** 497–510 (2012).

5. Jasin, M. & Rothstein, R. Repair of strand breaks by homologous recombination. *Cold Spring Harb. Perspect. Biol.* **5,** 1–18 (2013).

6. Aylon, Y., Liefshitz, B. & Kupiec, M. The CDK regulates repair of double-strand breaks by homologous recombination during the cell cycle. *EMBO J.* **23,** 4868–4875 (2004).

7. Hopfner, K. P., Putnam, C. D. & Tainer, J. A. DNA double-strand break repair from head to tail. *Curr. Opin. Struct. Biol.* **12,** 115–22 (2002).

8. Williams, R. S., Williams, J. S. & Tainer, J. A. Mre11-Rad50-Nbs1 is a keystone complex connecting DNA repair machinery, double-strand break signaling, and the chromatin template. *Biochem. Cell Biol.* **85,** 509–20 (2007).

9. Williams, G. J., Lees-Miller, S. P. & Tainer, J. A. Mre11-Rad50-Nbs1 conformations and the control of sensing, signaling, and effector responses at DNA double-strand breaks. *DNA Repair (Amst).* **9,** 1299–306 (2010).

10. Symington, L. S. Role of RAD52 epistasis group genes in homologous recombination and double-strand break repair. *Microbiol. Mol. Biol. Rev.* **66,** 630–70, table of contents (2002).

11. Berkovich, E., Monnat, R. J. & Kastan, M. B. Roles of ATM and NBS1 in chromatin structure modulation and DNA double-strand break repair. *Nat. Cell Biol.* **9,** 683–90 (2007).

12. Paull, T. T. & Gellert, M. Nbs1 potentiates ATP-driven DNA unwinding and endonuclease cleavage by the Mre11/Rad50 complex. *Genes Dev.* **13,** 1276–88

(1999).

13. Trujillo, K. M. & Sung, P. DNA structure-specific nuclease activities in the Saccharomyces cerevisiae Rad50*Mre11 complex. *J. Biol. Chem.* **276,** 35458–64 (2001).

14. Hopfner, K. P. *et al.* Structural biology of Rad50 ATPase: ATP-driven conformational control in DNA double-strand break repair and the ABC-ATPase superfamily. *Cell* **101,** 789–800 (2000).

15. Moreno-Herrero, F. *et al.* Mesoscale conformational changes in the DNA-repair complex Rad50/Mre11/Nbs1 upon binding DNA. *Nature* **437,** 440–3 (2005).

16. Lloyd, J. *et al.* A supramodular FHA/BRCT-repeat architecture mediates Nbs1 adaptor function in response to DNA damage. *Cell* **139,** 100–11 (2009).

17. Cerosaletti, K. M. *et al.* Retroviral expression of the NBS1 gene in cultured Nijmegen breakage syndrome cells restores normal radiation sensitivity and nuclear focus formation. *Mutagenesis* **15,** 281–6 (2000).

18. Lee, J.-H. & Paull, T. T. ATM activation by DNA double-strand breaks through the Mre11-Rad50-Nbs1 complex. *Science* **308,** 551–4 (2005).

19. Lavin, M. F. ATM and the Mre11 complex combine to recognize and signal DNA double-strand breaks. *Oncogene* **26,** 7749–7758 (2007).

20. Hartlerode, A. J., Morgan, M. J., Wu, Y., Buis, J. & Ferguson, D. O. Recruitment and activation of the ATM kinase in the absence of DNA-damage sensors. *Nat. Struct. Mol. Biol.* **22,** 736–43 (2015).

21. Tanaka, T., Halicka, H. D., Huang, X., Traganos, F. & Darzynkiewicz, Z. Constitutive histone H2AX phosphorylation and ATM activation, the reporters of DNA damage by endogenous oxidants. *Cell Cycle* **5,** 1940–5 (2006).

22. O'Donovan, P. J. & Livingston, D. M. BRCA1 and BRCA2: breast/ovarian cancer susceptibility gene products and participants in DNA double-strand break repair. *Carcinogenesis* **31,** 961–7 (2010).

23. Sodha, N., Mantoni, T. S., Tavtigian, S. V, Eeles, R. & Garrett, M. D. Rare germ line CHEK2 variants identified in breast cancer families encode proteins that show impaired activation. *Cancer Res.* **66,** 8966–70 (2006).

24. Falck, J., Mailand, N., Syljuåsen, R. G., Bartek, J. & Lukas, J. The ATM-Chk2-Cdc25A checkpoint pathway guards against radioresistant DNA synthesis. *Nature* **410,** 842–7 (2001).

25. Peng, C. Y. *et al.* Mitotic and G2 checkpoint control: regulation of 14-3-3 protein binding by phosphorylation of Cdc25C on serine-216. *Science* **277,** 1501–5

(1997).

26. Zhang, J. *et al.* Chk2 phosphorylation of BRCA1 regulates DNA double-strand break repair. *Mol. Cell. Biol.* **24,** 708–18 (2004).

27. Cortez, D., Wang, Y., Qin, J. & Elledge, S. J. Requirement of ATM-dependent phosphorylation of brca1 in the DNA damage response to double-strand breaks. *Science* **286,** 1162–6 (1999).

28. Meza, J. E., Brzovic, P. S., King, M. C. & Klevit, R. E. Mapping the functional domains of BRCA1. Interaction of the ring finger domains of BRCA1 and BARD1. *J. Biol. Chem.* **274,** 5659–65 (1999).

29. McCarthy, E. E., Celebi, J. T., Baer, R. & Ludwig, T. Loss of Bard1, the heterodimeric partner of the brca1 tumor suppressor, results in early embryonic lethality and chromosomal instability. *Mol. Cell. Biol.* **23,** 5056–5063 (2003).

30. Li, M. & Yu, X. Function of BRCA1 in the DNA damage response is mediated by ADP-Ribosylation. *Cancer Cell* **23,** 693–704 (2013).

31. Scully, R. *et al.* Association of BRCA1 with Rad51 in mitotic and meiotic cells. *Cell* **88,** 265–75 (1997).

32. Rogakou, E. P., Pilch, D. R., Orr, A. H., Ivanova, V. S. & Bonner, W. M. DNA double-stranded breaks induce histone H2AX phosphorylation on serine 139. *J. Biol. Chem.* **273,** 5858–68 (1998).

33. Rogakou, E. P., Boon, C., Redon, C. & Bonner, W. M. Megabase chromatin domains involved in DNA double-strand breaks in vivo. *J. Cell Biol.* **146,** 905–16 (1999).

34. Foray, N. *et al.* A subset of ATM- and ATR-dependent phosphorylation events requires the BRCA1 protein. *EMBO J.* **22,** 2860–71 (2003).

35. Yarden, R. I., Pardo-Reoyo, S., Sgagias, M., Cowan, K. H. & Brody, L. C. BRCA1 regulates the G2/M checkpoint by activating Chk1 kinase upon DNA damage. *Nat. Genet.* **30,** 285–9 (2002).

36. Saleh-Gohari, N. & Helleday, T. Strand invasion involving short tract gene conversion is specifically suppressed in BRCA2-deficient hamster cells. *Oncogene* **23,** 9136–41 (2004).

37. Zhang, F. *et al.* PALB2 links BRCA1 and BRCA2 in the DNA-damage response. *Curr. Biol.* **19,** 524–529 (2009).

38. Suwaki, N., Klare, K. & Tarsounas, M. RAD51 paralogs: roles in DNA damage signalling, recombinational repair and tumorigenesis. *Semin. Cell Dev. Biol.* **22,** 898–905 (2011).

39. Heyer, W.-D., Ehmsen, K. T. & Liu, J. Regulation of homologous recombination in eukaryotes. *Annu. Rev. Genet.* **44,** 113–39 (2010).

40. Thacker, J. The RAD51 gene family, genetic instability and cancer. *Cancer Lett.* **219,** 125–35 (2005).

41. Chun, J., Buechelmaier, E. S. & Powell, S. N. Rad51 paralog complexes BCDX2 and CX3 act at different stages in the BRCA1-BRCA2-dependent homologous recombination pathway. *Mol. Cell. Biol.* **33,** 387–395 (2013).

42. Thacker, J. The use of integrating DNA vectors to analyse the molecular defects in ionising radiation-sensitive mutants of mammalian cells including ataxia telangiectasia. *Mutat. Res.* **220,** 187–204

43. Cartwright, R., Tambini, C. E., Simpson, P. J. & Thacker, J. The XRCC2 DNA repair gene from human and mouse encodes a novel member of the recA/RAD51 family. *Nucleic Acids Res.* **26,** 3084–9 (1998).

44. Tambini, C. E., Spink, K. G., Ross, C. J., Hill, M. A. & Thacker, J. The importance of XRCC2 in RAD51-related DNA damage repair. *DNA Repair (Amst).* **9,** 517–25 (2010).

45. Meindl, A. *et al.* Germline mutations in breast and ovarian cancer pedigrees establish RAD51C as a human cancer susceptibility gene. *Nat. Genet.* **42,** 410–4 (2010).

46. Gao, L.-B. *et al.* RAD51 135G/C polymorphism and breast cancer risk: a meta-analysis from 21 studies. *Breast Cancer Res. Treat.* **125,** 827–35 (2011).

47. Loveday, C. *et al.* Germline mutations in RAD51D confer susceptibility to ovarian cancer. *Nat. Genet.* **43,** 879–82 (2011).

48. Loveday, C. *et al.* Germline RAD51C mutations confer susceptibility to ovarian cancer. *Nat. Genet.* **44,** 475–6; author reply 476 (2012).

49. Liu, N. XRCC2 is required for the formation of Rad51 Foci Induced by Ionizing Radiation and DNA cross-linking agent mitomycin C. *J. Biomed. Biotechnol.* **2,** 106–113 (2002).

50. Waltes, R. *et al.* Human RAD50 deficiency in a Nijmegen breakage syndrome-like disorder. *Am. J. Hum. Genet.* **84,** 605–16 (2009).

51. Shamseldin, H. E., Elfaki, M. & Alkuraya, F. S. Exome sequencing reveals a novel Fanconi group defined by XRCC2 mutation. *J. Med. Genet.* **49,** 184–6 (2012).

52. Park, J.-Y. *et al.* Complementation of hypersensitivity to DNA interstrand crosslinking agents demonstrates that XRCC2 is a Fanconi anaemia gene. *J. Med. Genet.* **53,** 672–80 (2016).

53. Gennery, A. R. *et al.* The clinical and biological overlap between Nijmegen breakage syndrome and Fanconi anemia. *Clin. Immunol.* **113,** 214–219 (2004).

54. Resnick, I. B. *et al.* Nijmegen breakage syndrome: clinical characteristics and mutation analysis in eight unrelated Russian families. *J. Pediatr.* **140,** 355–61 (2002).

55. Shimada, H. *et al.* First case of aplastic anemia in a Japanese child with a homozygous missense mutation in the NBS1 gene (I171V) associated with genomic instability. *Hum. Genet.* **115,** 372–6 (2004).

56. Ceccaldi, R. *et al.* Bone marrow failure in Fanconi anemia is triggered by an exacerbated p53/p21 DNA damage response that impairs hematopoietic stem and progenitor cells. *Cell Stem Cell* **11,** 36–49 (2012).

57. Garaycoechea, J. I. & Patel, K. J. Why does the bone marrow fail in Fanconi anemia? *Blood* **123,** 26–34 (2014).

58. Fundia, A., Gorla, N. & Larripa, I. Spontaneous chromosome aberrations in Fanconi's anemia patients are located at fragile sites and acute myeloid leukemia breakpoints. *Hereditas* **120,** 47–50 (1994).

59. Alter, B. P. Fanconi anemia and the development of leukemia. *Best Pract. Res. Clin. Haematol.* **27,** 214–21

60. Savage, S. A. & Dufour, C. Classical inherited bone marrow failure syndromes with high risk for myelodysplastic syndrome and acute myelogenous leukemia. *Semin. Hematol.* **54,** 105–114 (2017).

61. van der Burgt, I., Chrzanowska, K. H., Smeets, D. & Weemaes, C. Nijmegen breakage syndrome. *J. Med. Genet.* **33,** 153–6 (1996).

62. Digweed, M. & Sperling, K. Nijmegen breakage syndrome: clinical manifestation of defective response to DNA double-strand breaks. *DNA Repair (Amst).* **3,** 1207–17 (2004).

63. Kalb, R., Neveling, K., Nanda, I., Schindler, D. & Hoehn, H. Fanconi anemia: causes and consequences of genetic instability. *Genome Dyn.* **1,** 218–42 (2006).

64. Auerbach, A. D. Fanconi anemia and its diagnosis. *Mutat. Res.* **668,** 4–10 (2009).

65. Maraschio, P. *et al.* A novel mutation and novel features in Nijmegen breakage syndrome. *J. Med. Genet.* **38,** 113–7 (2001).

66. Chrzanowska, K. H. *et al.* Atypical clinical picture of the Nijmegen breakage syndrome associated with developmental abnormalities of the brain. *J. Med. Genet.* **38,** E3 (2001).

67. Chrzanowska, K. H., Gregorek, H., Dembowska-Bagińska, B., Kalina, M. A. & Digweed, M. Nijmegen breakage syndrome (NBS). *Orphanet J. Rare Dis.* **7,** 13 (2012).

68. Sklavos, M. M., Giri, N., Stratton, P., Alter, B. P. & Pinto, L. A. Anti-Müllerian hormone deficiency in females with Fanconi anemia. *J. Clin. Endocrinol. Metab.* **99,** 1608–14 (2014).

69. Chrzanowska, K. H. *et al.* High prevalence of primary ovarian insufficiency in girls and young women with Nijmegen breakage syndrome: evidence from a longitudinal study. *J. Clin. Endocrinol. Metab.* **95,** 3133–40 (2010).

70. Anur, P. *et al.* Late effects in patients with Fanconi anemia following allogeneic hematopoietic stem cell transplantation from alternative donors. *Bone Marrow Transplant.* **51,** 1–7 (2016).

71. Savitsky, K. *et al.* A single ataxia telangiectasia gene with a product similar to PI-3 kinase. *Science* **268,** 1749–53 (1995).

72. Stewart, G. S. *et al.* The DNA double-strand break repair gene hMRE11 is mutated in individuals with an ataxia-telangiectasia-like disorder. *Cell* **99,** 577–87 (1999).

73. Shiloh, Y. Ataxia-telangiectasia and the Nijmegen breakage syndrome: related disorders but genes apart. *Annu. Rev. Genet.* **31,** 635–62 (1997).

74. Luo, G. *et al.* Disruption of mRad50 causes embryonic stem cell lethality, abnormal embryonic development, and sensitivity to ionizing radiation. *Proc. Natl. Acad. Sci. U. S. A.* **96,** 7376–81 (1999).

75. Barbi, G. *et al.* Chromosome instability and X-ray hypersensitivity in a microcephalic and growth-retarded child. *Am. J. Med. Genet.* **40,** 44–50 (1991).

76. Bender, C. F. *et al.* Cancer predisposition and hematopoietic failure in Rad50(S/S) mice. *Genes Dev.* **16,** 2237–51 (2002).

77. Morales, M. *et al.* The Rad50S allele promotes ATM-dependent DNA damage responses and suppresses ATM deficiency: implications for the Mre11 complex as a DNA damage sensor. *Genes Dev.* **19,** 3043–54 (2005).

78. Sawyer, S. L. *et al.* Biallelic mutations in BRCA1 cause a new Fanconi anemia subtype. *Cancer Discov.* **5,** 135–42 (2015).

79. Wang, A. T. *et al.* A dominant mutation in human RAD51 reveals its function in DNA interstrand crosslink repair independent of homologous recombination. *Mol. Cell* **59,** 478–90 (2015).

80. Ameziane, N. *et al.* A novel Fanconi anaemia subtype associated with a dominant-negative mutation in RAD51. *Nat. Commun.* **6,** 8829 (2015).

81. Hira, A. *et al.* Mutations in the gene encoding the E2 conjugating enzyme UBE2T cause Fanconi anemia. *Am. J. Hum. Genet.* **96,** 1001–7 (2015).

82. Bluteau, D. *et al.* Biallelic inactivation of REV7 is associated with Fanconi anemia. *J. Clin. Invest.* **126,** 3580–4 (2016).

83. Meetei, A. R. *et al.* X-linked inheritance of Fanconi anemia complementation group B. *Nat. Genet.* **36,** 1219–24 (2004).

84. Noll, D. M., Mason, T. M. & Miller, P. S. Formation and repair of interstrand cross-links in DNA. *Chem. Rev.* **106,** 277–301 (2006).

85. Patrick, S. M., Tillison, K. & Horn, J. M. Recognition of cisplatin-DNA interstrand cross-links by replication protein A. *Biochemistry* **47,** 10188–96 (2008).

86. Rio, P. & Bueren, J. A. FA core complex moves to chromatin. *Blood* **111,** 4837–4838 (2008).

87. McHugh, P. J., Spanswick, V. J. & Hartley, J. A. Repair of DNA interstrand crosslinks: molecular mechanisms and clinical relevance. *Lancet. Oncol.* **2,** 483–90 (2001).

88. Niedernhofer, L. J. *et al.* The structure-specific endonuclease Ercc1-Xpf is required to resolve DNA interstrand cross-link-induced double-strand breaks. *Mol. Cell. Biol.* **24,** 5776–87 (2004).

89. Klein Douwel, D. *et al.* XPF-ERCC1 acts in Unhooking DNA interstrand crosslinks in cooperation with FANCD2 and FANCP/SLX4. *Mol. Cell* **54,** 460–71 (2014).

90. Howlett, N. G. *et al.* Biallelic inactivation of BRCA2 in Fanconi anemia. *Science* **297,** 606–9 (2002).

91. Seal, S. *et al.* Truncating mutations in the Fanconi anemia J gene BRIP1 are low-penetrance breast cancer susceptibility alleles. *Nat. Genet.* **38,** 1239–41 (2006).

92. Xia, B. *et al.* Fanconi anemia is associated with a defect in the BRCA2 partner PALB2. *Nat. Genet.* **39,** 159–61 (2007).

93. Vaz, F. *et al.* Mutation of the RAD51C gene in a Fanconi anemia-like disorder. *Nat. Genet.* **42,** 406–9 (2010).

94. Le Calvez-Kelm, F. *et al.* Rare, evolutionarily unlikely missense substitutions in CHEK2 contribute to breast cancer susceptibility: results from a breast cancer family registry case-control mutation-screening study. *Breast Cancer Res.* **13,** R6 (2011).

95. Park, D. J. *et al.* Rare mutations in XRCC2 increase the risk of breast cancer. *Am. J. Hum. Genet.* **90,** 734–9 (2012).

96. Damiola, F. *et al.* Rare key functional domain missense substitutions in MRE11A, RAD50, and NBN contribute to breast cancer susceptibility: results from a Breast Cancer Family Registry case-control mutation-screening study. *Breast Cancer Res.* **16,** R58 (2014).

97. Tavtigian, S. V *et al.* Rare, evolutionarily unlikely missense substitutions in ATM confer increased risk of breast cancer. *Am. J. Hum. Genet.* **85,** 427–46 (2009).

98. Goldgar, D. E. *et al.* Integrated evaluation of DNA sequence variants of unknown clinical significance: application to BRCA1 and BRCA2. *Am. J. Hum. Genet.* **75,** 535–44 (2004).

99. Goldgar, D. E. *et al.* Genetic evidence and integration of various data sources for classifying uncertain variants into a single model. *Hum. Mutat.* **29,** 1265–72 (2008).

100. Vallée, M. P. *et al.* Classification of missense substitutions in the BRCA genes: a database dedicated to Ex-UVs. *Hum. Mutat.* **33,** 22–8 (2012).

101. Thompson, B. A. *et al.* Calibration of multiple in silico tools for predicting pathogenicity of mismatch repair gene missense substitutions. *Hum. Mutat.* **34,** 255–65 (2013).

102. Titus, T. A. *et al.* The Fanconi anemia gene network is conserved from zebrafish to human. *Gene* **371,** 211–23 (2006).

103. Francia, S. *et al.* Site-specific DICER and DROSHA RNA products control the DNA-damage response. *Nature* **488,** 231–5 (2012).

104. Shive, H. R. *et al.* brca2 in zebrafish ovarian development, spermatogenesis, and tumorigenesis. *Proc. Natl. Acad. Sci. U. S. A.* **107,** 19350–5 (2010).

105. Rodríguez-Marí, A. *et al.* Roles of brca2 (fancd1) in oocyte nuclear architecture, gametogenesis, gonad tumors, and genome stability in zebrafish. *PLoS Genet.* **7,** e1001357 (2011).

106. Sharan, S. K. *et al.* Embryonic lethality and radiation hypersensitivity mediated by Rad51 in mice lacking Brca2. *Nature* **386,** 804–10 (1997).

107. Roeb, W., Higgins, J. & King, M.-C. Response to DNA damage of CHEK2 missense mutations in familial breast cancer. *Hum. Mol. Genet.* **21,** 2738–44 (2012).

108. Jou, C. J. *et al.* An in vivo cardiac assay to determine the functional consequences of putative long QT syndrome mutations. *Circ. Res.* **112,** 826–30 (2013).

109. Jou, C. J. *et al.* A functional assay for sick sinus syndrome genetic variants. *Cell. Physiol. Biochem.* **42,** 2021–2029 (2017).

110. Drost, M. *et al.* A cell-free assay for the functional analysis of variants of the mismatch repair protein MLH1. *Hum. Mutat.* **31,** 247–53 (2010).

111. Sorrells, S., Toruno, C., Stewart, R. A. & Jette, C. Analysis of apoptosis in zebrafish embryos by whole-mount immunofluorescence to detect activated Caspase 3. *J. Vis. Exp.* e51060 (2013). doi:10.3791/51060

112. Pereira, S. *et al.* Genotoxicity of acute and chronic gamma-irradiation on zebrafish cells and consequences for embryo development. *Environ. Toxicol. Chem.* **30,** 2831–7 (2011).

113. Liu, J. *et al.* Development of novel visual-plus quantitative analysis systems for studying DNA double-strand break repairs in zebrafish. *J. Genet. Genomics* **39,** 489–502 (2012).

114. Dahlem, T. J. *et al.* Simple methods for generating and detecting locus-specific mutations induced with TALENs in the zebrafish genome. *PLoS Genet.* **8,** e1002861 (2012).

115. Johnson, R. D., Liu, N. & Jasin, M. Mammalian XRCC2 promotes the repair of DNA double-strand breaks by homologous recombination. *Nature* **401,** 397–399 (1999).

116. Hilbers, F. S. *et al.* Rare variants in XRCC2 as breast cancer susceptibility alleles. *J. Med. Genet.* **49,** 618–20 (2012).

117. Pelttari, L. M. *et al.* RAD51, XRCC3, and XRCC2 mutation screening in Finnish breast cancer families. *Springerplus* **4,** 92 (2015).

118. Hilbers, F. S. *et al.* Functional analysis of missense variants in the putative breast cancer susceptibility gene XRCC2. *Hum. Mutat.* **37,** 914–25 (2016).

119. Scheckenbach, K., Wagenmann, M., Freund, M., Schipper, J. & Hanenberg, H. Squamous cell carcinomas of the head and neck in Fanconi anemia: risk, prevention, therapy, and the need for guidelines. *Klin. Padiatr.* **224,** 132–138 (2012).

120. Condie, A. *et al.* Analysis of the Fanconi anaemia complementation group A gene in acute myeloid leukaemia. *Leuk. Lymphoma* **43,** 1849–53 (2002).

121. Rodríguez-Marí, A. *et al.* Sex reversal in zebrafish fancl mutants is caused by Tp53-mediated germ cell apoptosis. *PLoS Genet.* **6,** e1001034 (2010).

122. Fu, C., Begum, K. & Overbeek, P. A. Primary ovarian insufficiency induced by fanconi anemia e mutation in a mouse model. *PLoS One* **11,** 1–13 (2016).

123. Alavattam, K. G. *et al.* Elucidation of the Fanconi anemia protein network in meoisis and its function in the regulation of histone modifications. *Cell Rep.* **17,** 1141–1157 (2016).

124. Simhadri, S. *et al.* Male fertility defect associated with disrupted BRCA1-PALB2 interaction in mice. *J. Biol. Chem.* **289,** 24617–29 (2014).

125. Botthof, J. G., Bielczyk-Maczyńska, E., Ferreira, L. & Cvejic, A. Loss of the homologous recombination gene rad51 leads to Fanconi anemia-like symptoms in zebrafish. *Proc. Natl. Acad. Sci. U. S. A.* **114,** E4452–E4461 (2017).

126. Sato, T., Endo, T., Yamahira, K., Hamaguchi, S. & Sakaizumi, M. Induction of female-to-male sex reversal by high temperature treatment in Medaka, Oryzias latipes. *Zoolog. Sci.* **22,** 985–8 (2005).

127. Schreeb, K. H., Groth, G., Sachsse, W. & Freundt, K. J. The karyotype of the zebrafish (Brachydanio rerio). *J. Exp. Anim. Sci.* **36,** 27–31 (1993).

128. Gornung, E., Gabrielli, I., Cataudella, S. & Sola, L. CMA3-banding pattern and fluorescence in situ hybridization with 18S rRNA genes in zebrafish chromosomes. *Chromosome Res.* **5,** 40–6 (1997).

129. Phillips, R. B. & Reed, K. M. Localization of repetitive DNAs to zebrafish (Danio rerio) chromosomes by fluorescence in situ hybridization (FISH). *Chromosome Res.* **8,** 27–35 (2000).

130. Liew, W. C. & Orbán, L. Zebrafish sex: a complicated affair. *Brief. Funct. Genomics* **13,** 172–87 (2014).

131. Slanchev, K., Stebler, J., de la Cueva-Méndez, G. & Raz, E. Development without germ cells: the role of the germ line in zebrafish sex differentiation. *Proc. Natl. Acad. Sci. U. S. A.* **102,** 4074–4079 (2005).

132. Siegfried, K. R. & Nüsslein-Volhard, C. Germ line control of female sex determination in zebrafish. *Dev. Biol.* **324,** 277–287 (2008).

133. Weidinger, G. *et al.* Dead end, a novel vertebrate germ plasm component, is required for zebrafish primordial germ cell migration and survival. *Curr. Biol.* **13,** 1429–34 (2003).

134. Dranow, D. B., Tucker, R. P. & Draper, B. W. Germ cells are required to maintain a stable sexual phenotype in adult zebrafish. *Dev. Biol.* **376,** 43–50 (2013).

135. Takatsu, K. *et al.* Induction of female-to-male sex change in adult zebrafish by aromatase inhibitor treatment. *Sci. Rep.* **3,** 3400 (2013).

136. Titus, T. A. *et al.* The Fanconi anemia/BRCA gene network in zebrafish: embryonic expression and comparative genomics. *Mutat. Res.* **668,** 117–32 (2009).

137. Rodríguez-Marí, A. & Postlethwait, J. H. The role of Fanconi anemia/BRCA genes in zebrafish sex determination. *Methods Cell Biol.* **105,** 461–90 (2011).

138. Berghmans, S. *et al.* Tp53 mutant zebrafish develop malignant peripheral nerve sheath tumors. *Proc Natl Acad Sci U S A* **102,** 407–412 (2005).

139. Parant, J. M., George, S. A., Holden, J. A. & Yost, H. J. Genetic modeling of Li-Fraumeni syndrome in zebrafish. *Dis. Model. Mech.* **3,** 45–56 (2010).

140. Lindeboom, R. G. H., Supek, F. & Lehner, B. The rules and impact of nonsense-mediated mRNA decay in human cancers. *Nat. Genet.* **48,** 1112–8 (2016).

141. Tang, R., Dodd, A., Lai, D., McNabb, W. C. & Love, D. R. Validation of zebrafish (Danio rerio) reference genes for quantitative real-time RT-PCR normalization. *Acta Biochim. Biophys. Sin. (Shanghai).* **39,** 384–390 (2007).

142. Rodríguez-Marí, A. *et al.* Characterization and expression pattern of zebrafish Anti-Müllerian hormone (Amh) relative to sox9a, sox9b, and cyp19a1a, during gonad development. *Gene Expr. Patterns* **5,** 655–67 (2005).

143. Guo, Y. *et al.* Gene structure, multiple alternative splicing, and expression in gonads of zebrafish Dmrt1. *Biochem. Biophys. Res. Commun.* **330,** 950–957 (2005).

144. Morais, R. D. V. S. *et al.* Thyroid hormone stimulates the proliferation of sertoli cells and single type A spermatogonia in adult zebrafish (danio rerio) testis. *Endocrinology* **154,** 4365–4376 (2013).

145. Thacker, J., Tambini, C. E., Simpson, P. J., Tsui, L. C. & Scherer, S. W. Localization to chromosome 7q36.1 of the human XRCC2 gene, determining sensitivity to DNA-damaging agents. *Hum. Mol. Genet.* **4,** 113–20 (1995).

146. Tambini, C. E. *et al.* The XRCC2 DNA repair gene: identification of a positional candidate. *Genomics* **41,** 84–92 (1997).

147. Liu, N. *et al.* XRCC2 and XRCC3, new human Rad51-family members, promote chromosome stability and protect against DNA cross-links and other damages. *Mol. Cell* **1,** 783–793 (1998).

148. Deans, B., Griffin, C. S., Maconochie, M. & Thacker, J. Xrcc2 is required for genetic stability, embryonic neurogenesis and viability in mice. *EMBO J.* **19,** 6675–6685 (2000).

149. Fu, C., Begum, K., Jordan, P. W., He, Y. & Overbeek, P. A. Dearth and delayed maturation of testicular germ cells in Fanconi anemia E mutant male mice. *PLoS One* **11,** e0159800 (2016).

150. van de Vrugt, H. J. *et al.* Evidence for complete epistasis of null mutations in

murine Fanconi anemia genes Fanca and Fancg. *DNA Repair (Amst).* **10,** 1252–61 (2011).

151. Klüver, N. *et al.* Differential expression of anti-Müllerian hormone (amh) and anti-Müllerian hormone receptor type II (amhrII) in the teleost Medaka. *Dev. Dyn.* **236,** 271–281 (2007).

152. von Hofsten, J., Larsson, A. & Olsson, P. E. Novel steroidogenic factor-1 homolog (ff1d) is coexpressed with anti-Mullerian hormone (AMH) in zebrafish. *Dev. Dyn.* **233,** 595–604 (2005).

153. Josso, N. *et al.* Anti-Müllerian hormone: the Jost factor. *Recent Prog. Horm. Res.* **48,** 1–59 (1993).

154. Lee, M. M. & Donahoe, P. K. Mullerian inhibiting substance: a gonadal hormone with multiple functions. *Endocr. Rev.* **14,** 152–64 (1993).

155. Miura, T., Miura, C., Konda, Y. & Yamauchi, K. Spermatogenesis-preventing substance in Japanese eel. *Development* **129,** 2689–2697 (2002).

156. Yoshinaga, N. *et al.* Sexually dimorphic expression of a teleost homologue of Müllerian inhibiting substance during gonadal sex differentiation in Japanese flounder, Paralichthys olivaceus. *Biochem. Biophys. Res. Commun.* **322,** 508–513 (2004).

157. Jamsai, D., O'Connor, A. E., O'Donnell, L., Lo, J. C. Y. & O'Bryan, M. K. Uncoupling of transcription and translation of Fanconi anemia (FANC) complex proteins during spermatogenesis. *Spermatogenesis* **5,** e979061

158. Wu, G.-C. *et al.* Testicular dmrt1 is involved in the sexual fate of the ovotestis in the protandrous black porgy. *Biol. Reprod.* **86,** 41–41 (2012).

159. Kobayashi, T. *et al.* Two DM domain genes, DMY and DMRT1, involved in testicular differentiation and development in the medaka, Oryzias latipes. *Dev. Dyn.* **231,** 518–26 (2004).

160. Kobayashi, T., Kajiura-Kobayashi, H., Guan, G. & Nagahama, Y. Sexual dimorphic expression of DMRT1 and Sox9a during gonadal differentiation and hormone-induced sex reversal in the teleost fish Nile tilapia (Oreochromis niloticus). *Dev. Dyn.* **237,** 297–306 (2008).

161. Veith, A.-M. *et al.* Cloning of the dmrt1 gene of Xiphophorus maculatus: dmY/dmrt1Y is not the master sex-determining gene in the platyfish. *Gene* **317,** 59–66 (2003).

162. Raymond, C. S., Murphy, M. W., O'Sullivan, M. G., Bardwell, V. J. & Zarkower, D. Dmrt1, a gene related to worm and fly sexual regulators, is required for mammalian testis differentiation. *Genes Dev.* **14,** 2587–95 (2000).

163. Nóbrega, R. H. *et al.* Fsh stimulates spermatogonial proliferation and differentiation in zebrafish via Igf3. *Endocrinology* **156,** 3804–3817 (2015).

164. Wang, D.-S. *et al.* Discovery of a gonad-specific IGF subtype in teleost. *Biochem. Biophys. Res. Commun.* **367,** 336–41 (2008).

165. Shive, H. R., West, R. R., Embree, L. J., Sexton, J. M. & Hickstein, D. D. Expression of KRAS G12V in zebrafish gills induces hyperplasia and CXCL8 - associated inflammation. *Zebrafish* **12,** 221–229 (2015).

166. Kliesch, S., Bergmann, M., Hertle, L., Nieschlag, E. & Behre, H. M. Semen parameters and testicular pathology in men with testicular cancer and contralateral carcinoma in situ or bilateral testicular malignancies. *Hum. Reprod.* **12,** 2830–5 (1997).

167. Botchan, A. *et al.* Testicular cancer and spermatogenesis. *Hum. Reprod.* **12,** 755–8 (1997).

168. Kooijman, R. Regulation of apoptosis by insulin-like growth factor (IGF)-I. *Cytokine Growth Factor Rev.* **17,** 305–23 (2006).

169. Neuvians, T. P. *et al.* Differential expression of IGF components and insulin receptor isoforms in human seminoma versus normal testicular tissue. *Neoplasia* **7,** 446–456 (2005).

170. Gil, T. *et al.* Testicular germ cell tumor: short and long-term side effects of treatment among survivors. *Mol. Clin. Oncol.* 258–264 (2016). doi:10.3892/mco.2016.960

171. Yoshimura, K., Yamauchi, T., Maeda, H. & Kawai, T. Cisplatin, vincristine, methotrexate, peplomycin, etoposide (COMPE) therapy for disseminated germ cell testicular tumors. *Int. J. Urol.* **4,** 47–51 (1997).

172. Litchfield, K. *et al.* Whole-exome sequencing reveals the mutational spectrum of testicular germ cell tumours. *Nat. Commun.* **6,** 5973 (2015).

173. Sonpavde, G., Hutson, T. E. & Roth, B. J. Management of recurrent testicular germ cell tumors. *Oncologist* **12,** 51–61 (2007).

174. Danoy, P., Sonoda, E., Lathrop, M., Takeda, S. & Matsuda, F. A naturally occurring genetic variant of human XRCC2 (R188H) confers increased resistance to cisplatin-induced DNA damage. *Biochem. Biophys. Res. Commun.* **352,** 763–8 (2007).

175. Sun, L., Nguyen, A. T., Spitsbergen, J. M. & Gong, Z. Myc-induced liver tumors in transgenic zebrafish can regress in tp53 null mutation. *PLoS One* **10,** 1–17 (2015).

176. Lu, J. W. *et al.* Liver-specific expressions of HBx and src in the p53 mutant trigger hepatocarcinogenesis in zebrafish. *PLoS One* **8,** 1–19 (2013).

177. Spitsbergen, J. M. & Kent, M. L. The state of the art of the zebrafish model for toxicology and toxicologic pathology research—advantages and current limitations. *Toxicol. Pathol.* **31,** 62–87 (2003).

178. Totoki, Y. *et al.* High-resolution characterization of a hepatocellular carcinoma genome. *Nat. Genet.* **43,** 464–469 (2011).

179. Wittwer, C. T. High-resolution DNA melting analysis: advancements and limitations. *Hum. Mutat.* **30,** 857–859 (2009).

180. Parant, J. M., George, S. A., Pryor, R., Wittwer, C. T. & Yost, H. J. A rapid and efficient method of genotyping zebrafish mutants. *Dev. Dyn.* **238,** 3168–74 (2009).

181. Thomas, H. R., Percival, S. M., Yoder, B. K. & Parant, J. M. High-throughput genome editing and phenotyping facilitated by high resolution melting curve analysis. *PLoS One* **9,** (2014).

182. Reyhanian Caspillo, N., Volkova, K., Hallgren, S., Olsson, P.-E. & Porsch-Hällström, I. Short-term treatment of adult male zebrafish (Danio Rerio) with 17α-ethinyl estradiol affects the transcription of genes involved in development and male sex differentiation. *Comp. Biochem. Physiol. C. Toxicol. Pharmacol.* **164,** 35–42 (2014).

183. Jørgensen, A., Morthorst, J. E., Andersen, O., Rasmussen, L. J. & Bjerregaard, P. Expression profiles for six zebrafish genes during gonadal sex differentiation. *Reprod. Biol. Endocrinol.* **6,** 25+ (2008).

184. Lamarche, B. J., Orazio, N. I. & Weitzman, M. D. The MRN complex in double-strand break repair and telomere maintenance. *FEBS Lett.* **584,** 3682–95 (2010).

185. Ogawa, H., Johzuka, K., Nakagawa, T., Leem, S. H. & Hagihara, A. H. Functions of the yeast meiotic recombination genes, MRE11 and MRE2. *Adv. Biophys.* **31,** 67–76 (1995).

186. Hopfner, K. P. *et al.* Structural biochemistry and interaction architecture of the DNA double-strand break repair Mre11 nuclease and Rad50-ATPase. *Cell* **105,** 473–85 (2001).

187. Petrini, J. H. J. & Stracker, T. H. The cellular response to DNA double-strand breaks: defining the sensors and mediators. *Trends Cell Biol.* **13,** 458–62 (2003).

188. Lilley, C. E., Schwartz, R. A. & Weitzman, M. D. Using or abusing: viruses and the cellular DNA damage response. *Trends Microbiol.* **15,** 119–26 (2007).

189. Stracker, T. H. & Petrini, J. H. J. The MRE11 complex: starting from the ends.

Nat. Rev. Mol. Cell Biol. **12,** 90–103 (2011).

190. Schwartz, R. A. *et al.* The Mre11/Rad50/Nbs1 complex limits adeno-associated virus transduction and replication. *J. Virol.* **81,** 12936–12945 (2007).

191. Czornak, K., Chughtai, S. & Chrzanowska, K. H. Mystery of DNA repair: the role of the MRN complex and ATM kinase in DNA damage repair. *J. Appl. Genet.* **49,** 383–96 (2008).

192. Heikkinen, K., Karppinen, S.-M., Soini, Y., Mäkinen, M. & Winqvist, R. Mutation screening of Mre11 complex genes: indication of RAD50 involvement in breast and ovarian cancer susceptibility. *J. Med. Genet.* **40,** e131 (2003).

193. Heikkinen, K. *et al.* RAD50 and NBS1 are breast cancer susceptibility genes associated with genomic instability. *Carcinogenesis* **27,** 1593–9 (2006).

194. Young, E. L. *et al.* Multigene testing of moderate-risk genes: be mindful of the missense. *J. Med. Genet.* **53,** 366–76 (2016).

195. Goodarzi, A. A. *et al.* ATM signaling facilitates repair of DNA double-strand breaks associated with heterochromatin. *Mol. Cell* **31,** 167–177 (2008).

196. Burma, S., Chen, B. P., Murphy, M., Kurimasa, A. & Chen, D. J. ATM phosphorylates histone H2AX in response to DNA double-strand breaks. *J. Biol. Chem.* **276,** 42462–7 (2001).

197. Saito, S. *et al.* ATM mediates phosphorylation at multiple p53 sites, including Ser(46), in response to ionizing radiation. *J. Biol. Chem.* **277,** 12491–4 (2002).

198. Westphal, C. H. Cell-cycle signaling: Atm displays its many talents. *Curr. Biol.* **7,** R789-92 (1997).

199. Matsuoka, S., Huang, M. & Elledge, S. J. Linkage of ATM to cell cycle regulation by the Chk2 protein kinase. *Science* **282,** 1893–7 (1998).

200. Chaturvedi, P. *et al.* Mammalian Chk2 is a downstream effector of the ATM-dependent DNA damage checkpoint pathway. *Oncogene* **18,** 4047–54 (1999).

201. Anderson, L., Henderson, C. & Adachi, Y. Phosphorylation and rapid relocalization of 53BP1 to nuclear foci upon DNA damage. *Mol. Cell. Biol.* **21,** 1719–29 (2001).

202. Carson, C. T. *et al.* The Mre11 complex is required for ATM activation and the G2/M checkpoint. *EMBO J.* **22,** 6610–20 (2003).

203. Uziel, T. *et al.* Requirement of the MRN complex for ATM activation by DNA damage. *EMBO J.* **22,** 5612–21 (2003).

204. Lee, J.-H. & Paull, T. T. Direct activation of the ATM protein kinase by the Mre11/Rad50/Nbs1 complex. *Science* **304,** 93–6 (2004).

205. Kim, S.-T., Xu, B. & Kastan, M. B. Involvement of the cohesin protein, Smc1, in Atm-dependent and independent responses to DNA damage. *Genes Dev.* **16,** 560–70 (2002).

206. Yazdi, P. T. *et al.* SMC1 is a downstream effector in the ATM/NBS1 branch of the human S-phase checkpoint. *Genes Dev.* **16,** 571–82 (2002).

207. Zhong, H., Bryson, A., Eckersdorff, M. & Ferguson, D. O. Rad50 depletion impacts upon ATR-dependent DNA damage responses. *Hum. Mol. Genet.* **14,** 2685–93 (2005).

208. Gatei, M. *et al.* ATM-dependent phosphorylation of nibrin in response to radiation exposure. *Nat. Genet.* **25,** 115–9 (2000).

209. Lim, D. S. *et al.* ATM phosphorylates p95/nbs1 in an S-phase checkpoint pathway. *Nature* **404,** 613–7 (2000).

210. Wu, X. *et al.* ATM phosphorylation of Nijmegen breakage syndrome protein is required in a DNA damage response. *Nature* **405,** 477–82 (2000).

211. Zhao, S. *et al.* Functional link between ataxia-telangiectasia and Nijmegen breakage syndrome gene products. *Nature* **405,** 473–7 (2000).

212. Bredemeyer, A. L. *et al.* ATM stabilizes DNA double-strand-break complexes during V(D)J recombination. *Nature* **442,** 466–70 (2006).

213. Bredemeyer, A. L., Huang, C.-Y., Walker, L. M., Bassing, C. H. & Sleckman, B. P. Aberrant V(D)J recombination in ataxia telangiectasia mutated-deficient lymphocytes is dependent on nonhomologous DNA end joining. *J. Immunol.* **181,** 2620–5 (2008).

214. Bredemeyer, A. L. *et al.* DNA double-strand breaks activate a multi-functional genetic program in developing lymphocytes. *Nature* **456,** 819–23 (2008).

215. Attarbaschi, A. *et al.* Non-Hodgkin lymphoma and pre-existing conditions: spectrum, clinical characteristics and outcome in 213 children and adolescents. *Haematologica* **101,** 1581–1591 (2016).

216. de Jager, M. & Kanaar, R. Genome instability and Rad50(S): subtle yet severe. *Genes Dev.* **16,** 2173–8 (2002).

217. Roset, R. *et al.* The Rad50 hook domain regulates DNA damage signaling and tumorigenesis. *Genes Dev.* **28,** 451–62 (2014).

218. Jacks, T. *et al.* Tumor spectrum analysis in p53-mutant mice. *Curr. Biol.* **4,** 1–7

(1994).

219. Hopkins, B. B. & Paull, T. T. The P. furiosus mre11/rad50 complex promotes 5' strand resection at a DNA double-strand break. *Cell* **135,** 250–60 (2008).

220. Mascarenhas, J. *et al.* Bacillus subtilis SbcC protein plays an important role in DNA inter-strand cross-link repair. *BMC Mol. Biol.* **7,** 20 (2006).

221. Djuzenova, C., Mühl, B., Schakowski, R., Oppitz, U. & Flentje, M. Normal expression of DNA repair proteins, hMre11, Rad50 and Rad51 but protracted formation of Rad50 containing foci in X-irradiated skin fibroblasts from radiosensitive cancer patients. *Br. J. Cancer* **90,** 2356–63 (2004).

222. Andegeko, Y. *et al.* Nuclear retention of ATM at sites of DNA double strand breaks. *J. Biol. Chem.* **276,** 38224–30 (2001).

223. Gatei, M. *et al.* ATM protein-dependent phosphorylation of Rad50 protein Regulates DNA repair and cell cycle control. *J. Biol. Chem.* **286,** 31542–31556 (2011).

224. Brown, K. D. *et al.* The ataxia-telangiectasia gene product, a constitutively expressed nuclear protein that is not up-regulated following genome damage. *Proc. Natl. Acad. Sci. U. S. A.* **94,** 1840–5 (1997).

225. So, S., Davis, A. J. & Chen, D. J. Autophosphorylation at serine 1981 stabilizes ATM at DNA damage sites. *J. Cell Biol.* **187,** 977–90 (2009).

226. Danilova, N. *et al.* The role of the DNA damage response in zebrafish and cellular models of diamond blackfan anemia. *Dis. Model. Mech.* **7,** 895–905 (2014).

227. Lipton, J. M. & Ellis, S. R. Diamond-blackfan anemia: diagnosis, treatment, and molecular pathogenesis. *Hematol. Oncol. Clin. North Am.* **23,** 261–282 (2009).

228. Traver, D. *et al.* Effects of lethal irradiation in zebrafish and rescue by hematopoietic cell transplantation. *Blood* **104,** 1298–305 (2004).

229. Thisse, C., Thisse, B., Schilling, T. F. & Postlethwait, J. H. Structure of the zebrafish snail1 gene and its expression in wild-type, spadetail and no tail mutant embryos. *Development* **119,** 1203–15 (1993).

230. Bertrand, J. Y. *et al.* Definitive hematopoiesis initiates through a committed erythromyeloid progenitor in the zebrafish embryo. *Development* **134,** 4147–56 (2007).

231. Jette, C. A. *et al.* BIM and other BCL-2 family proteins exhibit cross-species conservation of function between zebrafish and mammals. *Cell Death Differ.* **15,** 1063–72 (2008).

232. Travnickova, J. *et al.* Primitive macrophages control HSPC mobilization and definitive haematopoiesis. *Nat. Commun.* **6,** 6227 (2015).

233. Goody, M. F., Carter, E. V, Kilroy, E. A., Maves, L. & Henry, C. A. 'Muscling' throughout life: integrating studies of muscle development, homeostasis, and disease in zebrafish. *Curr. Top. Dev. Biol.* **124,** 197–234 (2017).

234. Muto, A. *et al.* Forward genetic analysis of visual behavior in zebrafish. *PLoS Genet.* **1,** e66 (2005).

235. Patton, E. E. & Zon, L. I. The art and design of genetic screens: zebrafish. *Nat. Rev. Genet.* **2,** 956–966 (2001).

236. Chakrabarti, S., Streisinger, G., Singer, F. & Walker, C. Frequency of gamma-ray induced specific locus and recessive lethal mutations in mature germ cells of the zebrafish, Brachydanio rerio. *Genetics* **103,** 109–23 (1983).

237. Lawson, N. D. & Wolfe, S. A. Forward and reverse genetic approaches for the analysis of vertebrate development in the zebrafish. *Dev. Cell* **21,** 48–64 (2011).

238. Christian, M. *et al.* Targeting DNA double-strand breaks with TAL effector nucleases. *Genetics* **186,** 757–61 (2010).

239. Sapranauskas, R. *et al.* The Streptococcus thermophilus CRISPR/Cas system provides immunity in Escherichia coli. *Nucleic Acids Res.* **39,** 9275–82 (2011).

240. Hwang, W. Y. *et al.* Efficient genome editing in zebrafish using a CRISPR-Cas system. *Nat. Biotechnol.* **31,** 227–9 (2013).

241. Ceccaldi, R. *et al.* Bone marrow failure in Fanconi anemia is triggered by an exacerbated p53/p21 DNA damage response that impairs hematopoietic stem and progenitor cells. *Cell Stem Cell* **11,** 36–49 (2012).

242. Hinz, J. M. Reduced apoptotic response to camptothecin in CHO cells deficient in XRCC3. *Carcinogenesis* **24,** 249–253 (2003).

243. Hakem, R., de la Pompa, J. L. & Mak, T. W. Developmental studies of Brca1 and Brca2 knock-out mice. *J. Mammary Gland Biol. Neoplasia* **3,** 431–45 (1998).

244. Ma, D., Zhang, J., Lin, H. -f., Italiano, J. & Handin, R. I. The identification and characterization of zebrafish hematopoietic stem cells. *Blood* **118,** 289–297 (2011).

245. Dephoure, N., Gould, K. L., Gygi, S. P. & Kellogg, D. R. Mapping and analysis of phosphorylation sites: a quick guide for cell biologists. *Mol. Biol. Cell* **24,** 535–542 (2013).

246. Garg, R. *et al.* Molecular cloning and characterization of the catalytic domain of zebrafish homologue of the ataxia-telangiectasia mutated gene. *Mol. Cancer Res.*

2, 348–53 (2004).

247. Leu, D. H. & Draper, B. W. The ziwi promoter drives germline-specific gene expression in zebrafish. *Dev. Dyn.* **239,** 2714–21 (2010).

248. Hartung, O., Forbes, M. M. & Marlow, F. L. Zebrafish vasa is required for germ-cell differentiation and maintenance. *Mol. Reprod. Dev.* **81,** 946–961 (2014).

249. Fan, L., Moon, J., Wong, T.-T., Crodian, J. & Collodi, P. Zebrafish primordial germ cell cultures derived from *vasa::RFP* transgenic embryos. *Stem Cells Dev.* **17,** 585–598 (2008).

250. Hjeij, R. *et al.* ARMC4 mutations cause primary ciliary dyskinesia with randomization of left/right body asymmetry. *Am. J. Hum. Genet.* **93,** 357–67 (2013).

251. Merveille, A.-C. *et al.* CCDC39 is required for assembly of inner dynein arms and the dynein regulatory complex and for normal ciliary motility in humans and dogs. *Nat. Genet.* **43,** 72–8 (2011).

252. Zariwala, M. A. *et al.* ZMYND10 is mutated in primary ciliary dyskinesia and interacts with LRRC6. *Am. J. Hum. Genet.* **93,** 336–45 (2013).

253. Davis, E. E., Frangakis, S. & Katsanis, N. Interpreting human genetic variation with in vivo zebrafish assays. *Biochim. Biophys. Acta - Mol. Basis Dis.* **1842,** 1960–1970 (2014).

254. Lindeman, R. E. & Pelegri, F. Vertebrate maternal-effect genes: insights into fertilization, early cleavage divisions, and germ cell determinant localization from studies in the zebrafish. *Mol. Reprod. Dev.* **77,** 299–313 (2010).

255. Mosimann, C. *et al.* Ubiquitous transgene expression and Cre-based recombination driven by the ubiquitin promoter in zebrafish. *Development* **138,** 169–77 (2011).

256. Mosimann, C. *et al.* Site-directed zebrafish transgenesis into single landing sites with the phiC31 integrase system. *Dev. Dyn.* **242,** 949–963 (2013).

257. Stemple, D. L. Structure and function of the notochord: an essential organ for chordate development. *Development* **132,** 2503–2512 (2005).

258. Hagmann, M. *et al.* Homologous recombination and DNA-end joining reactions in zygotes and early embryos of zebrafish (Danio rerio) and Drosophila melanogaster. *Biol. Chem.* **379,** 673–81 (1998).

259. Dai, J., Cui, X., Zhu, Z. & Hu, W. Non-homologous end joining plays a key role in transgene concatemer formation in transgenic zebrafish embryos. *Int. J. Biol. Sci.* **6,** 756–68 (2010).

260. Howe, K. *et al.* The zebrafish reference genome sequence and its relationship to the human genome. *Nature* **496,** 498–503 (2013).

261. Bunting, S. F. *et al.* 53BP1 inhibits homologous recombination in Brca1-deficient cells by blocking resection of DNA breaks. *Cell* **141,** 243–54 (2010).

262. Deng, C.-X. Roles of BRCA1 in DNA damage repair: a link between development and cancer. *Hum. Mol. Genet.* **12,** 113R–123 (2003).

263. Chen, C.-C. *et al.* ATM loss leads to synthetic lethality in BRCA1 BRCT mutant mice associated with exacerbated defects in homology-directed repair. *Proc. Natl. Acad. Sci. U. S. A.* **114,** 7665–7670 (2017).

264. Schulte-Merker, S. & Stainier, D. Y. R. Out with the old, in with the new: reassessing morpholino knockdowns in light of genome editing technology. *Development* **141,** 3103–3104 (2014).

265. Kok, F. O. *et al.* Reverse genetic screening reveals poor correlation between morpholino-induced and mutant phenotypes in zebrafish. *Dev. Cell* **32,** 97–108 (2015).

266. Stainier, D. Y. R., Kontarakis, Z. & Rossi, A. Making sense of anti-sense data. *Dev. Cell* **32,** 7–8 (2015).

267. Blum, M., De Robertis, E. M., Wallingford, J. B. & Niehrs, C. Morpholinos: Antisense and Sensibility. *Dev. Cell* **35,** 145–149 (2015).

268. Wu, J., Lu, L.-Y. & Yu, X. The role of BRCA1 in DNA damage response. *Protein Cell* **1,** 117–123 (2010).

269. Wolters, S. *et al.* Loss of Caenorhabditis elegans BRCA1 promotes genome stability during replication in smc-5 mutants. *Genetics* **196,** 985–99 (2014).

270. Lafarge, S. & Montané, M.-H. Characterization of Arabidopsis thaliana ortholog of the human breast cancer susceptibility gene 1: AtBRCA1, strongly induced by gamma rays. *Nucleic Acids Res.* **31,** 1148–55 (2003).

271. Saha, J. & Davis, A. J. Unsolved mystery: the role of BRCA1 in DNA end-joining. *J. Radiat. Res.* **57,** i18–i24 (2016).

272. Wu, W. *et al.* HERC2 is an E3 ligase that targets BRCA1 for degradation. *Cancer Res.* **70,** 6384–92 (2010).

273. Li, M. & Yu, X. Function of BRCA1 in the DNA damage response is mediated by ADP-ribosylation. *Cancer Cell* **23,** 693–704 (2013).